



# Gas Emissions From the Western Aleutians Volcanic Arc

Tobias P. Fischer<sup>1\*</sup>, Taryn M. Lopez<sup>2</sup>, Alessandro Aiuppa<sup>3</sup>, Andrea L. Rizzo<sup>4</sup>, Tehnuka Ilanko<sup>5</sup>, Katherine A. Kelley<sup>6</sup> and Elizabeth Cottrell<sup>7</sup>

<sup>1</sup>Department of Earth and Planetary Sciences, University of New Mexico, Albuquerque, NM, United States, <sup>2</sup>Geophysical Institute, University of Alaska Fairbanks, Fairbanks, AK, United States, <sup>3</sup>Dipartimento di Scienze Della Terra e Del Mare, Università di Palermo, Palermo, Italy, <sup>4</sup>Istituto Nazionale di Geofisica e Vulcanologia, Sezione di Palermo, Palermo, Italy, <sup>5</sup>Te Aka Mātua - School of Science, University of Waikato, Hamilton, New Zealand, <sup>6</sup>Graduate School of Oceanography, University of Rhode Island, Washington County, RI, United States, <sup>7</sup>Department of Mineral Sciences, National Museum of Natural History, Smithsonian Institution, Washington, VA, United States

## OPEN ACCESS

### Edited by:

Antonio Paonita,  
Istituto Nazionale di Geofisica e  
Vulcanologia (INGV), Italy

### Reviewed by:

Franco Tassi,  
University of Florence, Italy  
Phillipson Bani,  
UMR6524 Laboratoire Magmas et  
Volcans (LMV), France

### \*Correspondence:

Tobias P. Fischer  
fischer@unm.edu

### Specialty section:

This article was submitted to  
Volcanology,  
a section of the journal  
Frontiers in Earth Science

**Received:** 29 September 2021

**Accepted:** 18 November 2021

**Published:** 06 December 2021

### Citation:

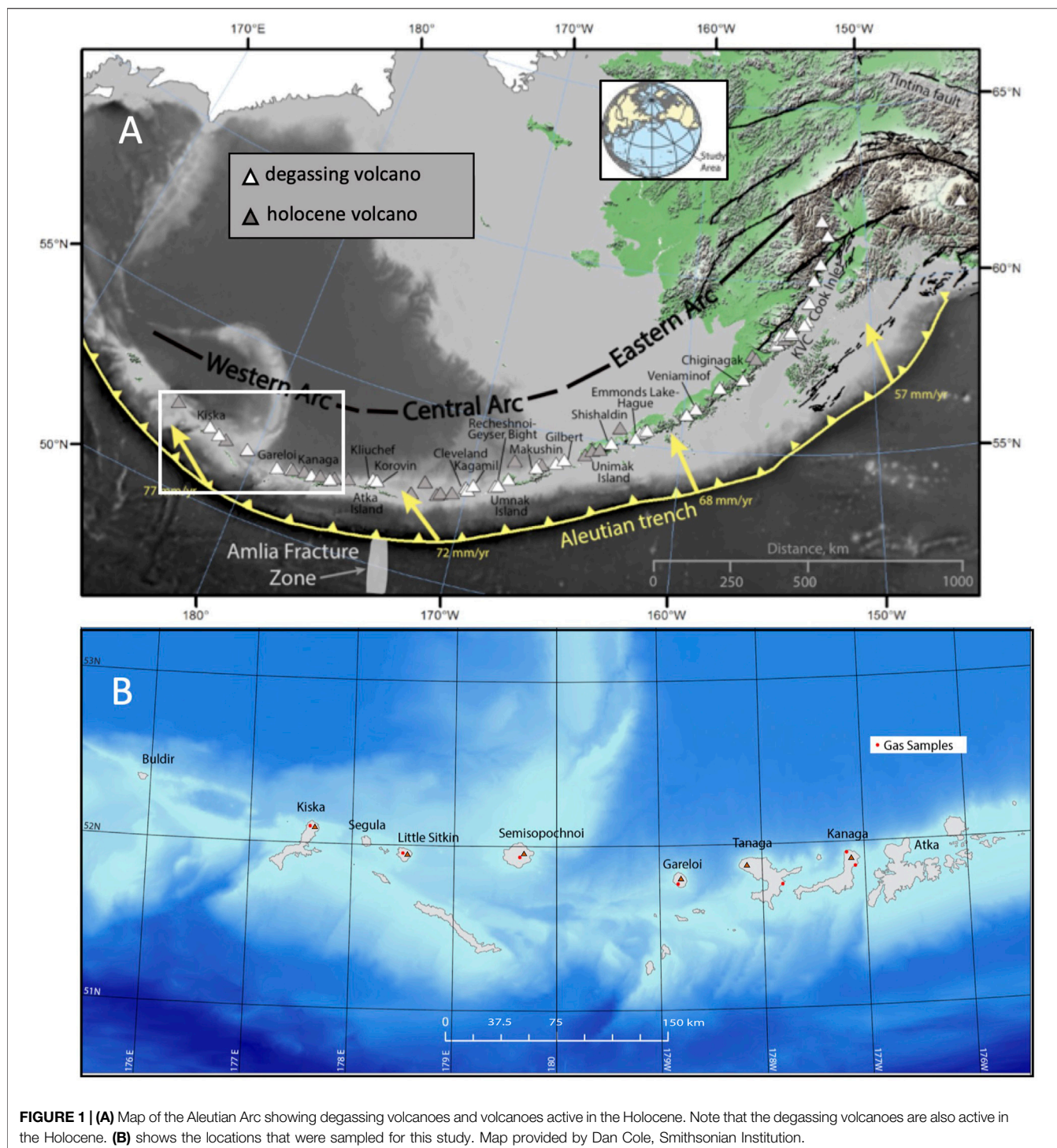
Fischer TP, Lopez TM, Aiuppa A,  
Rizzo AL, Ilanko T, Kelley KA and  
Cottrell E (2021) Gas Emissions From  
the Western Aleutians Volcanic Arc.  
*Front. Earth Sci.* 9:786021.  
doi: 10.3389/feart.2021.786021

The Aleutian Arc is remote and highly active volcanically. Its 4,000 km extent from mainland Alaska to Russia's Kamchatka peninsula hosts over 140 volcanic centers of which about 50 have erupted in historic times. We present data of volcanic gas samples and gas emission measurements obtained during an expedition to the western-most segment of the arc in September 2015 in order to extend the sparse knowledge on volatile emissions from this remote but volcanically active region. Some of the volcanoes investigated here have not been sampled for gases before this writing. Our data show that all volcanoes host high-temperature magmatic-hydrothermal systems and have gas discharges typical of volcanoes in oceanic arcs. Based on helium isotopes, the western Aleutian Arc segment has minimal volatile contributions from the overriding crust. Volcanic CO<sub>2</sub> fluxes from this arc segment are small, compared to the emissions from volcanoes on the Alaska Peninsula and mainland Alaska. The comparatively low CO<sub>2</sub> emissions may be related to the lower sediment flux delivered to the trench in this part of the arc.

**Keywords:** Aleutians, volcano, gas, volatiles, geochemistry

## INTRODUCTION

The Aleutian Arc is one of the most volcanically active and remote arcs in the world. The arc extends ~4,000 km from mainland Alaska to Russia's Kamchatka Peninsula and separates the Bering Sea to the North from the Pacific Ocean to the South (**Figure 1**). The eastern 2,500 km of the arc represents the region of active volcanism and is undergoing subduction of the Pacific plate beneath the North American plate. The arc has ~142 volcanic centers, of which 54 volcanoes have been historically active (Cameron et al., 2020). At the time of writing (2021), Semisopchnoi, Great Sitkin and Pavlof volcanoes are currently erupting, and Gareloi and Cleveland volcanoes have shown signs of unrest (GVP, 2015; GVP, 2019; GVP, 2021a; GVP, 2021b; GVP, 2021c; GVP, 2021d). The type of volcanic activity is highly variable throughout the arc, with eruptions ranging from nearly continuous Strombolian-style basaltic eruptions (e.g. Pavlof 2014) to infrequent, discrete Plinian events such as the 1912 Katmai/Novarupta eruption (Fierstein and Hildreth, 1992). The frequent eruptions occurring in the Aleutian Arc often produce high-altitude ash clouds that are hazardous to the numerous aircraft that fly over the North Pacific Ocean. Previous studies have investigated volcanic gas emissions from many Eastern and Central Aleutian volcanoes; however at the time of this study little was known about volcanic gas emissions from the Western Aleutian volcanoes.



We characterize volcanic gas emissions from the sparsely studied and highly remote Western Aleutians volcanic islands (from west to east) of Kiska, Little Sitkin, Semisopchnoi, Gareloi, Tanaga and Kanaga (**Figure 1B**). These volcanoes are all considered to be historically active by the Alaska Volcano Observatory, defined as having a known or suspected eruption, persistent fumaroles, a volcanic deformation signal,

and/or seismic swarm of volcanic origin since 1700 (Cameron et al., 2020). Because the Western Aleutians volcanoes are some of the most remote in Alaska, many eruptions in this region have been poorly documented throughout historic time and little is known in general about these volcanic systems.

In this publication we present the first constraints on the chemical composition of volcanic gases from Western Aleutians



**FIGURE 2** | Examples of degassing features in the Western Aleutians. **A:** Fumarole at the flank of Kiska Volcano with native sulfur deposits. The fumarole seen here is about 10 m in diameter and the plume is about 100 m tall. **B:** Fumaroles (100–270°C) at the summit of Gareloi volcano. The fumarole field is about 100 m wide. **C:** Hot spring (62°C) on the flanks of Tanaga volcano; **D:** Fumaroles (boiling temperature) at summit of Kanaga Volcano.

volcanoes of Gareloi, Kiska and Kanaga. We also present new measurements from hydrothermal gas discharges from Semisopochnoi, Tanaga and Little Sitkin volcanoes to complement previous studies. We targeted these volcanoes during an expedition that was jointly supported by NSF, the USGS and the Deep Carbon Observatory in 2015 and involved transportation by a combination of boat, helicopter and foot to reach most of the volcanic centers. Prior to this study, several field efforts since the 1980s have been aimed at measuring volatile emissions within the Aleutian Arc, including collection and analysis of Eastern and Central Aleutian volcanic gas and water samples for chemical and isotopic composition (Motyka et al., 1993; Symonds et al., 2003a; Symonds et al., 2003b; Evans et al., 2015); annual to bi-weekly surveys of plume composition and flux for volcanoes within the Cook Inlet and Katmai Volcanic Cluster regions were performed by Alaska Volcano Observatory scientists (Casadevall et al., 1994; Gerlach et al., 1994; Doukas, 1995; Doukas and McGee, 2007; McGee et al., 2010; Werner et al., 2011; Werner et al., 2013) and targeted gas composition and flux measurements at the individual volcanoes of Akutan (Bergfeld et al., 2013), Ukinrek-Maars (Evans et al., 2009) and Mount Martin, Mount Mageik, and Trident (Lopez et al., 2017). While these studies provide significant information on volcanic gas discharges from the Aleutians and the processes controlling the compositions of these emissions, the main degassing features from the Western Aleutian arc segment were virtually uncharacterized before this work. We also present the first  $\text{SO}_2$  flux measurements obtained from Gareloi and Kiska volcanoes. Together, these new constraints on volcanic gas composition and flux allow us to make inferences about the subsurface volcanic systems and current state of volcanic activity at these remote

volcanoes. The Western Aleutians, like other remote island arcs that are built on oceanic crust (i.e. Kuril, Izu-Bonin Marianas), have gas compositions that appear to be minimally affected by contributions from the overriding arc crust, providing a relatively undistorted view into slab- and mantle-derived volatiles.

## MATERIALS AND METHODS

### Volcano Settings

**Figure 1B** shows the location of Western Aleutian volcanoes sampled in this study and **Figure 2** shows some of their fumaroles and thermal features. Kiska Volcano is the westernmost historically active volcano within the Aleutian Arc (**Figure 1B**). Kiska is a stratovolcano with volcanic rocks of basaltic to andesitic composition (Miller et al., 1998). Confirmed historic eruptions consisted of ash and gas emissions in 1990 and lava effusion in 1962, 1964, 1969 and 1990 (<https://volcano.si.edu/volcano.cfm?vn=31102>). Other reported volcanic activity has comprised primarily volcanic gas emissions. This study sampled volcanic fluids from Kiska Volcano (52.1056 N, 177.5994 E, 1,049 m) that were emanating from a roaring ~10 m diameter fumarole vent on the upper west flank of the volcanic edifice. The vent consisted of a depression containing ~10–20 vigorously-degassing and audibly-jetting fumaroles whose emissions coalesced into a coherent plume (**Figure 2A**). The ground surrounding the vent was yellow in color and contained native sulfur deposits. The apparent high gas flux and confined emission location prevented safe access to sample the fumaroles by inserting a titanium tube directly into the vents when we visited this site.

Due to this situation, we were able to approach the site only to collect a gas sample from the plume above the vents that was affected by atmospheric contamination.

Little Sitkin volcano is a stratovolcano within a system of nested calderas (Miller et al., 1998). No confirmed eruptions from Little Sitkin have occurred in historic time, though observations are limited for this remote location. Volcanic rocks are primarily andesitic in composition, and range from basalt to dacite (Snyder, 1959; Larsen et al., 2020). Gas emissions from Little Sitkin emanate primarily from a geothermal region located on the western flank of the volcanic edifice (51.96117 N, 178.49226 E, 166 m), and this was the target of our study. Gas emissions in this region were released via three degassing manifestations: fumarolic emissions, bubbling springs and mud pools. Fumarolic regions near the summit and the northwest shore of the island have been previously reported (Snyder, 1959), but were not sampled during this study.

Semisopochnoi island is composed of scattered volcanic vents, the prominent caldera of Semisopochnoi volcano, and older, ancestral volcanic rocks. Volcanic rocks on Semisopochnoi range from basalt to dacite in composition (Miller et al., 1998; Coombs et al., 2007). Reports of volcanic eruptions prior to our 2015 field study occurred in 1772, 1790, 1792, 1830, 1873, and 1987 (<https://volcano.si.edu/volcano.cfm?vn=311060>) The 1987 eruption occurred from the extracaldera Sugarloaf Peak. Since 2018 Semisopochnoi has been undergoing intermittent eruptive activity from Mount Cerberus (GVP, 2021d). At the time of our study the volcano was in a period of quiescence, with no persistent fumaroles present to our knowledge. Water samples were collected from a warm spring next to Fenner Creek in the caldera with no visible bubbles (51.93636 N, 179.65459 E, 1,332 m).

Gareloi volcano is a stratovolcano comprising two overlapping volcanic edifices, referred to as the South and North Peaks, respectively. It is one of the most active volcanoes of the Western Aleutians with at least nine confirmed eruptions since 1791 (<https://volcano.si.edu/volcano.cfm?vn=311070>). Gareloi has also had persistent abundant seismicity since a seismic network was installed in 2005 (Coombs et al., 2008). Gareloi's erupted products are potassium rich in composition and range primarily from shoshonite to latite in composition, with sparse andesite (Coombs et al., 2012). Gareloi's largest historical eruption occurred in 1929 (Coombs et al., 2008) and likely formed the South Peak's asymmetrical crater that opens to the southeast. The South Peak Crater (51.7646 N, 178.80697 W, 1,326 m) is the home of the primary degassing region on Gareloi, an active fumarole field on the crater wall, whose gas emissions coalesce into a coherent plume (**Figure 2B**). These gases were targeted during this study. The North Peak contains a steeply walled crater that was observed to contain a crater lake and potentially an active fumarole field at the lake's edge at the time of our study, but was not targeted here.

Tanaga Island is home to three volcanic centers: Tanaga, Sajaka and Takawangha. Of these Tanaga is thought to be the youngest and only historically active vent of the three. The only confirmed historic eruption from Tanaga occurred in 1914, with suspected eruptions occurring in 1773–1770, 1791 and 1829

([www.alaska.edu](http://www.alaska.edu)). Little information is available on these eruptions, and they may have originated from the other volcanic centers (Miller et al., 1998). The erupted products from the three volcanic centers range from basalt to dacite in composition. While no known fumarole fields exist on Tanaga Island, natural hot springs (**Figure 2C**) are located on the edge of Hot Springs Bay (51.77175 N, 177.79955 W, 1 m), southeast of Takawangha. These hot springs were targeted during our study.

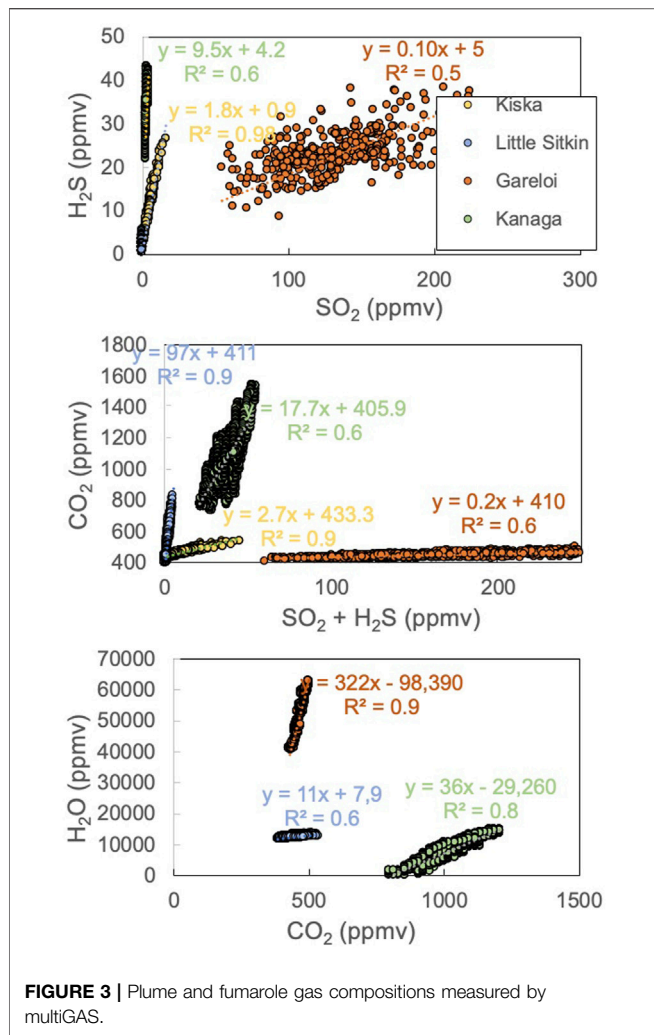
Kanaga volcano is the easternmost volcano discussed here. It is a stratovolcano within an older caldera on the north end of Kanaga island (Miller et al., 1998). Kanaga has had several confirmed historic eruptions including 1786, 1904, 1906, 1942, 1994–95 and most recently in 2012 (GVP, 2013). Erupted products range from basalt to andesite. Volcanic fluids from Kanaga Volcano (51.9230167 N, 177.161083 W, 1,237 m) were released from two main sources in 2015: 1) numerous individual fumaroles dispersed along the ~10 m wide southwest to southeast trending fracture that has dissected the summit since its 2012 eruption (**Figure 2D**); and 2) hot springs located ~7.3 km southeast of the summit. Yellow sulfur deposits surround the active fumaroles and travertine deposits are prominent in the hot springs region.

## Sampling and Analytical Techniques

We utilized a number of techniques for the collection of gas samples depending on the specific situation at the volcano. When possible, we collected direct gas samples from vents or bubbling springs in the crater or on the volcano's flanks using pre-evacuated Giggenbach bottles containing NaOH (Giggenbach and Goguel, 1989b). Where vents were not accessible, we measured plume gas composition by Multi-GAS (Aiuppa et al., 2005) and collected gas samples in Tedlar Bags for immediate subsequent carbon isotope analysis by Infrared Isotope Ratio Analyzer (Delta Ray) located on our boat (Rizzo et al., 2014; Fischer and Lopez, 2016). If there was a substantial plume, we made SO<sub>2</sub> flux measurements using a miniDOAS system (Galle et al., 2002) from the ground or helicopter. We collected water and gas samples from hot springs where no fumaroles were present or accessible.

Direct fumarole sampling involves inserting a titanium tube into a volcanic vent and drawing gases directly into previously evacuated glass bottles (i.e. Giggenbach bottles). The bottles contain a 5N NaOH solution that absorbs the acid gases (CO<sub>2</sub>, SO<sub>2</sub>, H<sub>2</sub>S, HCl, HF) and water vapor allowing the non-reactive gases (noble gases, H<sub>2</sub>, N<sub>2</sub>, O<sub>2</sub>, CH<sub>4</sub>, CO) to accumulate in the head space. This technique has been described in Giggenbach and Goguel (1989a) and more recently in Oppenheimer et al. (2014). Gas and water samples were also collected in copper tubes clamped or crimped at both ends for noble gas analyses (Sano and Fischer, 2013). The gas composition of Giggenbach bottles was analyzed in the Volatiles Laboratory at UNM using a combination of gas chromatography and quadrupole mass spectrometry following established procedures (de Moor et al., 2013a; Lee et al., 2017; Ilanko et al., 2019).

Helium isotopes were analyzed in splits from the Giggenbach bottles or from separately collected copper tubes. The samples were analyzed in the noble gases isotope laboratory at INGV,



Sezione di Palermo (Italy), following the analytical procedures outlined in e.g. Rizzo et al. (2016). The  $^3\text{He}/^4\text{He}$  ratio is expressed as  $R/R_a$  (where  $R_a$  is the ratio in air and equal to  $1.39 \times 10^{-6}$ ) and was corrected for air contamination ( $R_c/R_a$ ) using the  $\text{He}/\text{Ne}$  ratio following the equation proposed by Sano et al. (1987).

Nitrogen isotopes were analyzed for select gas samples at the University of New Mexico using a stable isotope ratio mass spectrometer with gas bench following the techniques described in Ilanko et al. (2019). Air standards were analyzed every 3–4 analyses to correct raw  $\delta^{15}\text{N}$  values. A blank was also run for each sample or air standard and the peak areas were subtracted from those subsequently measured in the sample. The blank-corrected air values were then subtracted from the blank-corrected sample values. Reported errors are given in 1 s.d. over 4–6 peaks. Although the number of peaks for calculations varies between samples, the same peak numbers were used for the blank corrections and the air standard associated with each sample. Unfortunately, as shown in the results section,  $\delta^{15}\text{N}$  values for these samples are burdened with high standard deviations due to interferences with unidentified peaks or low signals, making the data of limited value.

Water samples for water anion and cation analyses were collected at warm and hot spring sites using standard collection procedure that involved transfer of water into a 60 ml plastic syringe, and filtering through 0.2 micron millipore filters into Nalgene bottles. Samples were analyzed at the analytical chemistry laboratory in the Department of Earth and Planetary Sciences at the University of New Mexico using established IC and ICP OES methods (i.e. ASTM 300.1 and US EPA 200.7).

## Multi-GAS

The Multi-GAS used in the work was provided by Alessandro Aiuppa (University of Palermo) and was equipped with an infrared  $\text{CO}_2$  sensor and electrochemical sensors for  $\text{SO}_2$  and  $\text{H}_2\text{S}$  (Aiuppa et al., 2014). The sensor unit was placed close to the fumarolic vents in campaign style while other samples were collected, usually for 1–2 h. The derived concentration data (acquired at 0.5 Hz) were post-processed to derive ratios between volatile species, using a routine procedure (Aiuppa et al., 2014). In brief, co-acquired gas concentration data for pairs of gas species were compared in scatter plots (see Figure 3), and the gas/gas ratios were derived from the slopes of the best fit linear regression lines for each volcano's dataset.

## miniDOAS

The miniDOAS used in this work follows the design and approach of Galle et al. (2002) and has previously been used at Anatahan volcano, Mariana Islands (Hilton et al., 2007) at Erta Ale volcano, Ethiopia and Masaya, Nicaragua (de Moor et al., 2013b). The data processing is performed using DOASIS software (Kraus, 2006) that enables real-time calculation of the plume  $\text{SO}_2$  burden. The  $\text{SO}_2$  burden combined with constraints on windspeed allow emission rates to be calculated (Stoiber et al., 1983). At Kiska Volcano we performed several walking traverses along the crater rim on September 10 and measured wind-speed using a hand-held anemometer at the same time we measured plume  $\text{SO}_2$  burden. At Gareloi we mounted the miniDOAS in the helicopter with the telescope positioned vertically out the small window and performed flight traverses under the plume on September 14 at an average altitude of 470 m above sea level. We had measured wind speed using the wind circle method (Doukas, 2002) during a previous trip to the summit (September 13) and asked the pilot to estimate wind speed during the flight. At Kanaga we performed a helicopter traverse as well as a walking traverse and constrained wind speed via the wind circle method at the same time as the plume  $\text{SO}_2$  burden measurements (September 21). During the walking traverse, we were only able to partially capture the plume, due to inaccessible terrain.

## RESULTS

Generally speaking, our results presented in this section show that the  $\text{SO}_2$  fluxes were quite low and typical for volcanoes at a low state of activity (Fischer et al., 2019; Werner et al., 2019). Gas discharges are dominated by  $\text{H}_2\text{O}$ , followed by  $\text{CO}_2$  and the sulfur species. Except for Gareloi, which has a fumarole temperature up

**TABLE 1** | Gas chemical composition in mmol/mol total gas. All samples were collected in September 2015.

| Volcano/sample ID           | Temp. °C | H <sub>2</sub> O | CO <sub>2</sub> | S <sub>f</sub> | SO <sub>2</sub> | H <sub>2</sub> S | HCl   | HF     | He     | H <sub>2</sub> | Ar    | O <sub>2</sub> | N <sub>2</sub> | CH <sub>4</sub> | CO      |
|-----------------------------|----------|------------------|-----------------|----------------|-----------------|------------------|-------|--------|--------|----------------|-------|----------------|----------------|-----------------|---------|
| Kanaga Fum 1a S21           | 95       | 921.03           | 34.55           | 3.60           | 2.13            | 1.47             | 0.09  | <0.001 | 0.0015 | 0.561          | 0.624 | 0.001          | 39.54          | 0.00082         | 0.00081 |
| Kanaga Fum 1b S27           | 95       | 971.58           | 9.059           | n.a            | n.a             | n.a              | n.a   | n.a    | 0.0007 | 0.267          | 0.289 | 0.008          | 18.79          | 0.00039         | 0.00039 |
| Kanaga Fum 2a S10           | n.d      | 908.06           | 24.71           | 0.44           | 0.41            | 0.03             | 2.08  | <0.001 | 0.0008 | 0.124          | 0.693 | 11.90          | 51.99          | <0.0002         | <0.0002 |
| Kanaga Fum 2 S11            | n.d      | 927.51           | 14.97           | n.d            | n.d             | n.d              | 1.89  | <0.001 | 0.0007 | 0.044          | 0.452 | 8.028          | 47.11          | <0.0002         | <0.0002 |
| Gareloy Fum 1a S1           | 102      | 985.51           | 1.982           | 7.17           | 5.81            | 1.36             | 2.80  | 0.001  | 0.0001 | 1.572          | 0.013 | 0.000          | 0.935          | 0.00400         | 0.01195 |
| Gareloy Fum 1b S14          | 102      | 983.52           | 4.130           | 7.47           | 5.99            | 1.48             | 2.11  | 0.001  | 0.0001 | 1.512          | 0.015 | 0.000          | 1.232          | 0.01358         | 0.00025 |
| Gareloy Fum 2a S8           | 270      | 983.46           | 4.185           | 10.1           | 9.05            | 1.07             | 0.60  | 0.27   | 0.0001 | 0.697          | 0.006 | 0.015          | 0.647          | 0.00458         | 0.00012 |
| Gareloy Fum 2b S29          | 270      | 953.64           | 11.30           | 28.1           | 24.1            | 4.02             | 0.40  | 0.45   | 0.0004 | 3.003          | 0.037 | 0.000          | 3.024          | 0.02407         | 0.00170 |
| Little Sitkin 1a S5         | 66       | 795.80           | 164.9           | 10.7           | 0.96            | 9.74             | 0.65  | <0.001 | 0.0231 | 0.808          | 0.050 | 0.093          | 20.10          | 6.84929         | <0.0002 |
| Little Sitkin BS2 S26       | 55       | 446.49           | 492.4           | 16.2           | 0.84            | 15.4             | 0.32  | <0.001 | 0.0209 | 1.194          | 0.184 | 0.054          | 32.10          | 11.0480         | <0.0002 |
| Little Sitkin Fum 1a S3     | 97       | 893.18           | 98.00           | 1.91           | 0.24            | 1.66             | 0.07  | <0.001 | 0.0030 | 0.148          | 0.013 | 0.000          | 5.148          | 1.52506         | <0.0002 |
| Little Sitkin Fum 1b S9     | 97       | 878.77           | 115.0           | n.a            | n.a             | n.a              | n.a   | n.a    | 0.0054 | 0.172          | 0.016 | 0.000          | 4.324          | 1.72416         | <0.0002 |
| Kiska Fumarole KIF1 S16     | n.d      | 536.94           | 44.59           | 8.77           | n.a             | n.a              | 11.96 | <0.001 | 0.0059 | <0.001         | 2.258 | 69.76          | 325.7          | <0.0002         | <0.0002 |
| Tanaga Hot Spring Gas 1 S22 | 62       | 970.00           | 1.048           | 0.16           | n.a             | n.a              | 1.41  | <0.001 | 0.0001 | <0.001         | 0.043 | 1.336          | 4.727          | <0.0002         | <0.0002 |

n.a, not analyzed; n.d. not determined.

**TABLE 2** | Noble gas and nitrogen stable isotopes.

|  | Noble gases |        |                   |        |   | Nitrogen |                   |      |
|--|-------------|--------|-------------------|--------|---|----------|-------------------|------|
|  | R/Ra        | He/Ne  | Rc/Ra             | +/-    | Ar <sup>40</sup> /Ar <sup>36</sup> corr | +/-      | δ <sup>15</sup> N | ±    |
| Kanaga Fum 1a S21                        | 5.95        | 1.1    | 7.96              | 0.0662 | 295.32                                  | 0.16     | -0.42             | 0.10 |
| Kanaga Fum 1b S27                        | 5.99        | 1.13   | 7.93              | 0.0657 | 294.61                                  | 0.16     | -0.45             | 0.08 |
| Kanaga Fum 1c <sup>a</sup>               | 5.76        | 0.95   | 8.14              | 0.0589 | 295.55                                  | 0.15     | —                 | —    |
| Kanaga Fum 2a S10                        | n.a         | n.a    | —                 | —      | n.a                                     | —        | 0.39              | 0.12 |
| Kanaga Fum 2 S11                         | n.a         | n.a    | —                 | —      | n.a                                     | —        | 0.30              | 0.09 |
| Gareloy Fum 1a S1                        | 7.76        | 5.88   | 8.15              | 0.0658 | 295.31                                  | 0.07     | -1.59             | 0.76 |
| Gareloy Fum 1b S14 <sup>a</sup>          | 7.71        | 3.82   | 8.31              | 0.0674 | 293.85                                  | 0.26     | -1.63             | 1.01 |
| Gareloy Fum 2a S8                        | 6.80        | 4.74   | 7.22              | 0.0581 | 279.03                                  | 0.08     | —                 | —    |
| Gareloy Fum 2b S29 <sup>a</sup>          | 6.91        | 6.63   | 7.20 <sup>a</sup> | 0.0515 | 294.19                                  | 0.21     | —                 | —    |
| Little Sitkin 1a S5 <sup>a,b</sup>       | 0.88        | 0.35   | n.d               | —      | 297.67                                  | 0.16     | —                 | —    |
| Little Sitkin BS2 S26                    | 7.08        | 93.12  | 7.10              | 0.0557 | 299.30                                  | 0.09     | —                 | —    |
| Little Sitkin Fum 1a S3                  | 7.02        | 325.44 | 7.02              | 0.0566 | 301.19                                  | 0.09     | —                 | —    |
| Little Sitkin Fum 1b S9                  | n.a         | n.a    | —                 | —      | n.a                                     | —        | —                 | —    |
| Kiska Fumarole KIF1 S16                  | n.a         | n.a    | —                 | —      | n.a                                     | —        | —                 | —    |
| Tanaga Hot Spring Gas 1 S22 <sup>b</sup> | 0.97        | 0.39   | n.d               | —      | 296.16                                  | 0.15     | —                 | —    |

<sup>a</sup>Noble gas isotopes and He/Ne from Cu tube.

<sup>b</sup>Heavily air contaminated samples - unreliable values due to analytical issues.

**TABLE 3** | Multi GAS data collected in September 2015.

|               | Molar ratios                    |                                  |                                  |                                   |                                 |                                  |                                  | mole %                            |                  |                 |                 |                  |
|---------------|---------------------------------|----------------------------------|----------------------------------|-----------------------------------|---------------------------------|----------------------------------|----------------------------------|-----------------------------------|------------------|-----------------|-----------------|------------------|
|               | H <sub>2</sub> /SO <sub>2</sub> | H <sub>2</sub> S/SO <sub>2</sub> | CO <sub>2</sub> /SO <sub>2</sub> | CO <sub>2</sub> /H <sub>2</sub> S | CO <sub>2</sub> /S <sub>T</sub> | H <sub>2</sub> O/SO <sub>2</sub> | H <sub>2</sub> O/CO <sub>2</sub> | H <sub>2</sub> O/H <sub>2</sub> S | H <sub>2</sub> O | CO <sub>2</sub> | SO <sub>2</sub> | H <sub>2</sub> S |
| Kiska         | Nd                              | 1.8                              | 6.9                              | 3.8                               | 2.5                             | nd                               | Nd                               | nd                                | —                | 71              | 10.3            | 18.6             |
| Little Sitkin | Nd                              | nd                               | nd                               | 98                                | 98                              | nd                               | 11                               | 1,078                             | 91.6             | 8.3             | —               | 0.08             |
| Gareloi       | 0.11                            | 0.1                              | 0.26                             | 2.6                               | 0.2                             | 83                               | 320                              | 832                               | 98.4             | 0.3             | 1.2             | 0.12             |
| Kanaga        | Nd                              | 9.5                              | 186                              | 19.6                              | 18                              | 6,696                            | 36                               | 705                               | 97.1             | 2.7             | 0.015           | 0.14             |

to 270°C and displays a magmatic gas composition, all other volcanoes discharge gases that have a mixed magmatic-hydrothermal character. Helium isotopes of gas samples are within the MOR range (Graham, 2002) implying no or only minor contributions of radiogenic helium from the overriding crust. CO<sub>2</sub>-N<sub>2</sub>-<sup>3</sup>He relative abundances allow for the assessment of the contributions of these volatiles from of from the mantle

wedge and subducted materials (Sano and Marty, 1995; Sano et al., 2001). Our data of gas chemistry are consistent with minor slab-derived volatile contributions to a predominantly mantle-derived source for CO<sub>2</sub> and N<sub>2</sub>. A detailed evaluation of the carbon contributions from the subducted slab and how it varies along the entire Aleutian volcanic arc is presented in Lopez et al. (in prep.). The results from direct gas samples are shown in

**TABLE 4** | SO<sub>2</sub> fluxes measured by miniDOAS and calculated CO<sub>2</sub> fluxes using indicated gas ratios from direct samples or MultiGAS.

|         | SO <sub>2</sub><br>flux<br>t/day | ±   | MG     | Direct | MG                | Direct            | SO <sub>2</sub><br>(mol/yr) | CO <sub>2</sub><br>(mol/yr) | CO <sub>2</sub><br>(mol/yr)         | CO <sub>2</sub><br>(Tg/yr)          | ±       |
|---------|----------------------------------|-----|--------|--------|-------------------|-------------------|-----------------------------|-----------------------------|-------------------------------------|-------------------------------------|---------|
|         | —                                | —   | C/St M | C/St M | C/SO <sub>2</sub> | C/SO <sub>2</sub> | —                           | MG CO <sub>2</sub> /St      | MG CO <sub>2</sub> /SO <sub>2</sub> | MG CO <sub>2</sub> /SO <sub>2</sub> | —       |
| Kanaga  | 70                               | 30  | 18     | 9.6    | 186.0             | 16.2              | 12,775                      | 229,950                     | 2,376,150                           | 1.05E-04                            | 4.5E-05 |
|         | —                                | —   | —      | 56.5   | —                 | 60.5              | —                           | —                           | —                                   | —                                   | —       |
| Gareloi | 320                              | 80  | 0.20   | 0.28   | 0.20              | 0.34              | 58,400                      | 11,680                      | 11,680                              | 5.1E-07                             | 1.3E-07 |
|         | —                                | —   | —      | 0.55   | —                 | 0.69              | —                           | —                           | —                                   | —                                   | —       |
|         | —                                | —   | —      | 0.41   | —                 | 0.46              | —                           | —                           | —                                   | —                                   | —       |
|         | —                                | —   | —      | 0.40   | —                 | 0.47              | —                           | —                           | —                                   | —                                   | —       |
| Kiska   | 3.6                              | 0.1 | 2.5    | 5.09   | 6.9               | n.d               | 657                         | 1,643                       | 4,533                               | 2.0E-07                             | 6E-08   |
| Total   | —                                | —   | —      | —      | —                 | —                 | —                           | —                           | —                                   | 0.00011                             | 0.00004 |

Tables 1 and 2, water chemistry of spring samples is in **Supplementary Table S1** and the results of the Multi-GAS and SO<sub>2</sub> flux measurements are shown in **Table 3** and **Table 4**, respectively.

### Direct Samples of Gas and Water Phase

The complete gas chemistry is shown in **Table 1** and compositions are typical of magmatic and hydrothermal gas discharges from volcanoes in arc settings (Fischer and Chiodini, 2015). We obtained gas samples from the plume formed above the fumarolic vents at Kiska (unknown temperature), Little Sitkin (97°C), Gareloi (102°C and 270°C), and Kanaga (95°C). We also obtained gas samples from bubbling hot springs at Little Sitkin (55°C and 66°C) and Tanaga (62°C). The sample from Kiska is heavily air contaminated and is not discussed further because we have reliable Multi-GAS data for this plume/vent. All fumarole gases are dominated by H<sub>2</sub>O (879–986 mmol/mol), followed by CO<sub>2</sub> (4–115 mmol/mol) and total Sulfur (S<sub>t</sub> = SO<sub>2</sub> + H<sub>2</sub>S, 0.4–28 mmol/mol). Kanaga and Gareloi had comparatively high HCl contents of up to 2 mmol/mol. Trace gases include He, H<sub>2</sub>, CH<sub>4</sub>, CO. CH<sub>4</sub> reached up to 1.7 mmol/mol at Little Sitkin. The gases from bubbling springs and extracted from the water phase are dominated by CO<sub>2</sub> with minor H<sub>2</sub>S and CH<sub>4</sub>.

Noble gas and nitrogen isotope data are reported in **Table 2**. The <sup>3</sup>He/<sup>4</sup>He ratios corrected for air contamination range from 7.0 to 8.3 R<sub>a</sub>. These values are within the MORB range (8 ± 1 R<sub>a</sub>; Graham (2002), and at the high end of values typical for arc volcanoes (Hilton et al., 2002; Sano and Fischer, 2013). Although the Gareloi samples are somewhat air contaminated, with He/Ne of 3.8–6.6, the corrected value of 8.3 R<sub>a</sub> approaches some of the highest measured values at arcs to date: 8.6 R<sub>a</sub> at Goryachii Klyuch in the Kurile Islands (Taran, 2009; Tolstikhin, 1986), 8.8 R<sub>a</sub> at Galeras Volcano, Colombia, although the latter sample is highly air contaminated, resulting in a large correction (Sano et al., 1997), and 9.0 R<sub>a</sub> at Pacaya volcano, Guatemala, in olivine-hosted fluid inclusions (Battaglia et al., 2018). The helium isotope ratios of our samples indicate that the Western Aleutian volcanoes are among the least influenced by crustal helium of any arc volcano. Two samples from bubbling springs at Tanaga and Little Sitkin are heavily air contaminated and not further discussed. The

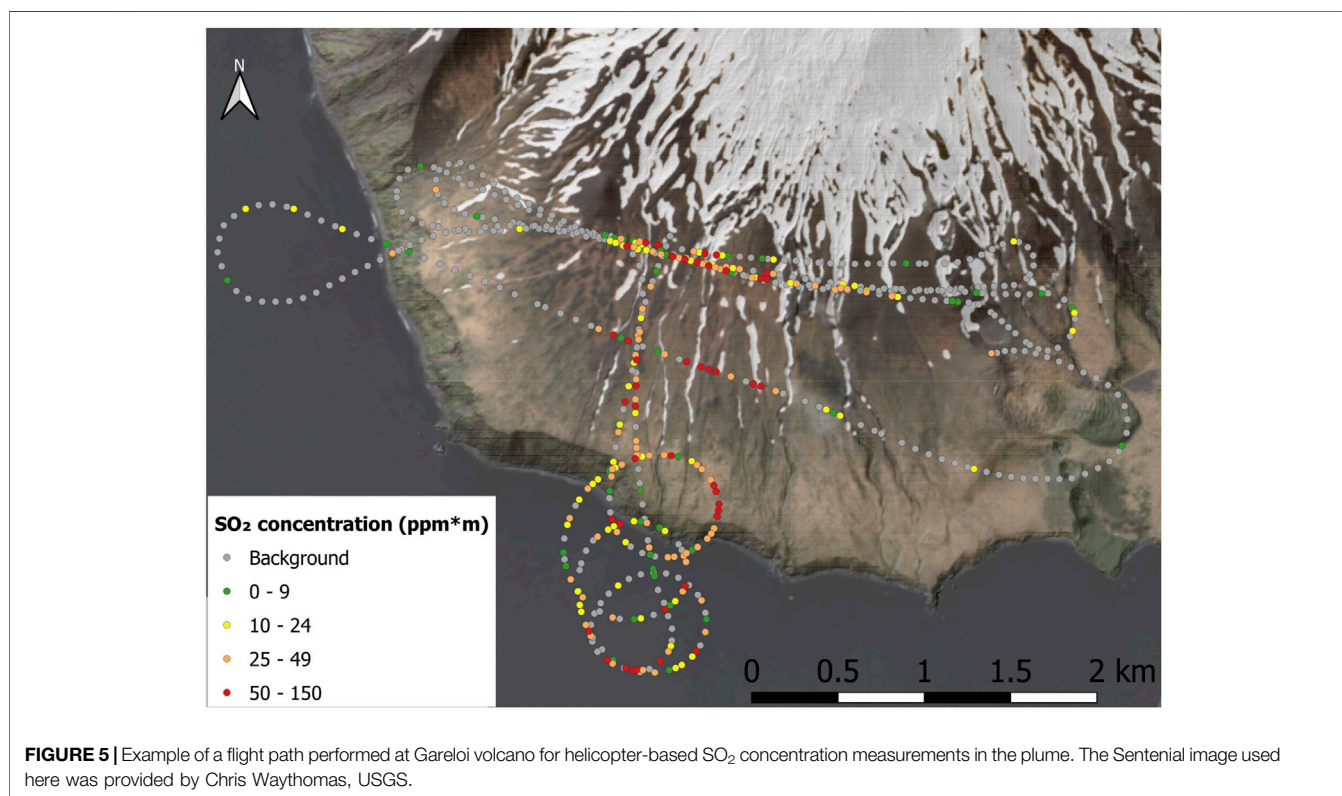
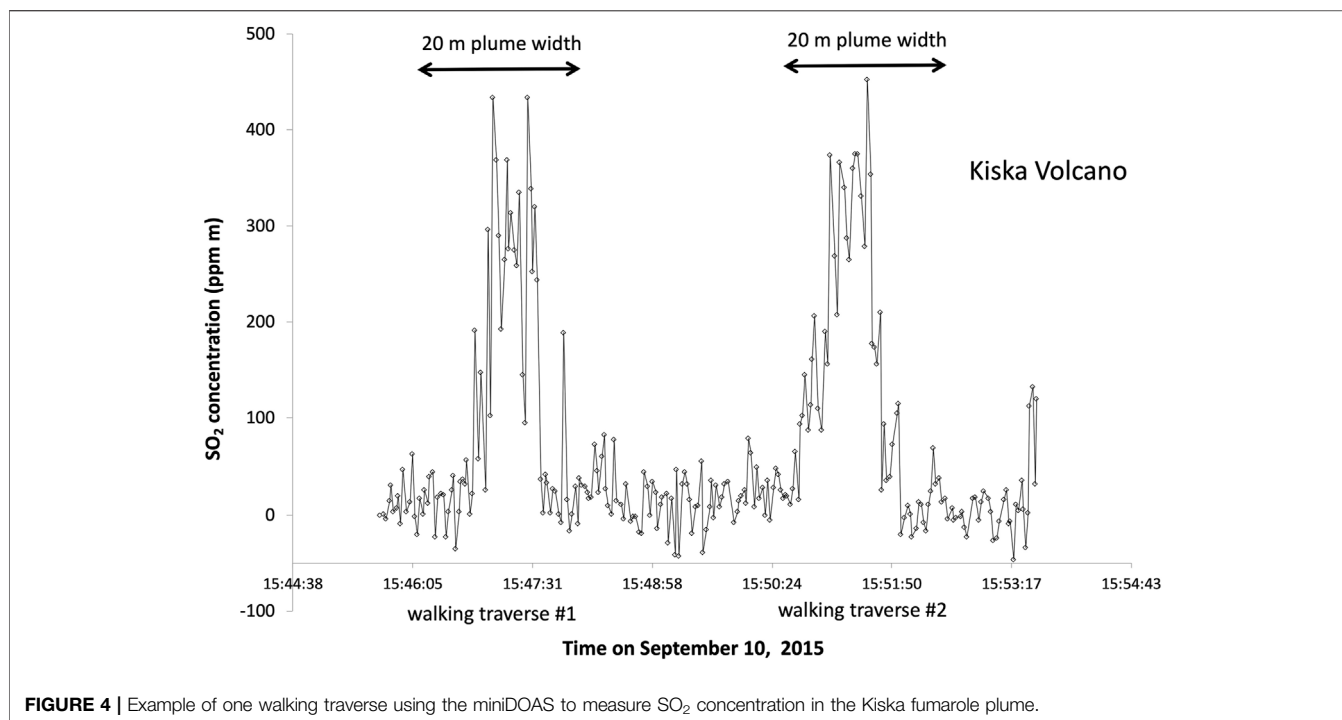
<sup>40</sup>Ar/<sup>36</sup>Ar ratios of gas samples are similar to the air value of 295 with the highest ratio reaching 301, typical of arc gases (Sano and Fischer, 2013). As can be seen from **Table 2**, duplicate samples (e.g. Gareloi Fum 1a and 1b; and 2a and 2b) from the same fumarole with one collected in a Cu-tube and the other in a Giggenbach bottle, followed by splitting in the lab, have indistinguishable He- and Ar- isotope values. This underscores the notion that both types of samples are valid for noble gas isotope sampling; however, if highly acid gases are sampled, Cu-tubes are better to be clamped in the field, rather than cold-welded (Sano and Fischer, 2013).

Nitrogen isotope data were only obtained from two localities. The Kanaga fumaroles have values of δ<sup>15</sup>N from -0.4 to +0.4‰, consistent with significant air contamination (δ<sup>15</sup>N<sub>air</sub> = 0.0‰) while the Gareloi fumarole gas has a value of -1.6 ± 0.9‰, also within error of air but potentially more negative. As mentioned above, these analyses were burdened with significant analytical issues, due to low signal and unidentified peaks resulting in high standard deviations, making them of limited value.

Water cation and anion data are shown in **Supplementary Table S1**. We collected water samples from springs on Kanaga, Little Sitkin, Semisopochnoi and Tanaga. Prior to our expedition, the only reported water sample data were from Semisopochnoi and Little Sitkin (Evans et al., 2015). Water temperatures range from 23°C for Semisopochnoi to 86°C at Kanaga, pH varies from acid at Little Sitkin to neutral at Semisopochnoi. Kanaga and Tanaga springs are located on the volcanoes' flanks and characterized by high Na, K, and Ca values while Semisopochnoi and Little Sitkin springs are located within the volcanoes' craters or calderas and characterized by lower, Na, K, and Ca values. SO<sub>4</sub> contents are highest at Little Sitkin and Cl is highest at Tanaga and Kanaga.

### Multi-GAS Major Gas Ratios

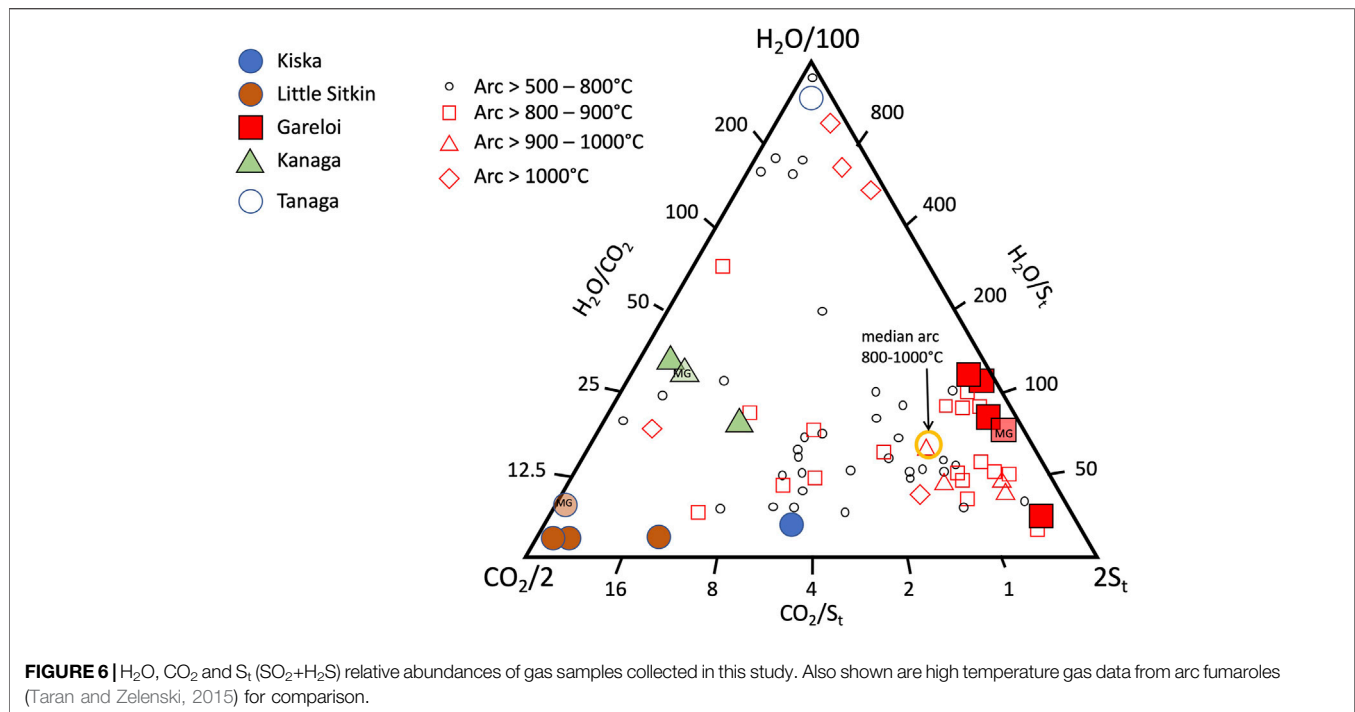
We obtained Multi-GAS data from Kiska, Little Sitkin, Gareloi and Kanaga volcanoes. The results are shown in **Table 3**. Consistent with direct gas samples, the dominant gas species is H<sub>2</sub>O, followed by CO<sub>2</sub> or SO<sub>2</sub>. CO<sub>2</sub>/S<sub>t</sub> ratios show a wide range from 0.2 at the high-temperature vents of Gareloi to 98 at the low-temperature hydrothermal system of Little Sitkin. Kiska (2.5) and Kanaga (18) have intermediate CO<sub>2</sub>/S<sub>t</sub> ratios. Notably, at Gareloi,



the amount of SO<sub>2</sub> detected by Multi-GAS in the gas plume was higher than the mean fumarole composition, resulting in lower average H<sub>2</sub>O/SO<sub>2</sub> of 83 than that of the direct gas samples

(average H<sub>2</sub>O/SO<sub>2</sub> = 120). We were not able to reliably measure H<sub>2</sub>O at Kanaga. **Figure 3** shows the Multi-GAS correlation plots with R<sup>2</sup> values as a measure of data quality.





## SO<sub>2</sub> Fluxes

We successfully obtained SO<sub>2</sub> fluxes from Gareloi and Kanaga by helicopter traverse and from Kiska by walking traverse. The SO<sub>2</sub> flux data are summarized in **Table 4** and **Figure 4** shows an example of the two walking traverses performed at Kiska volcano.

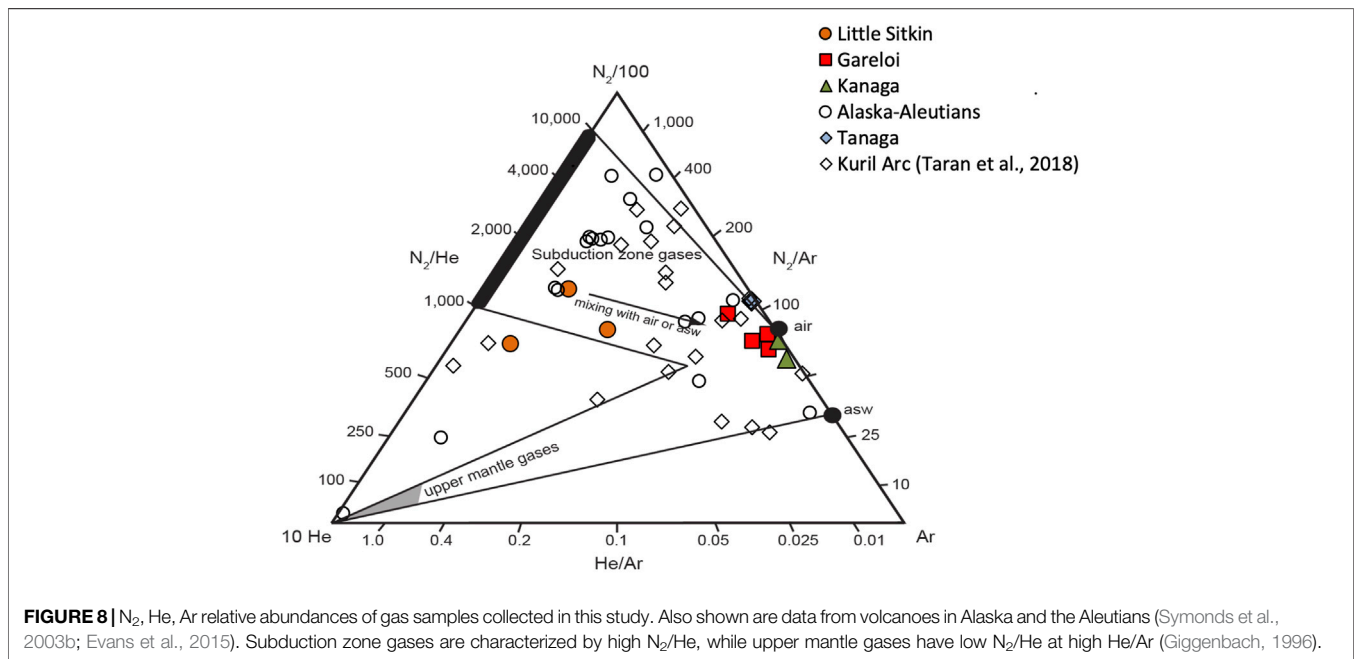
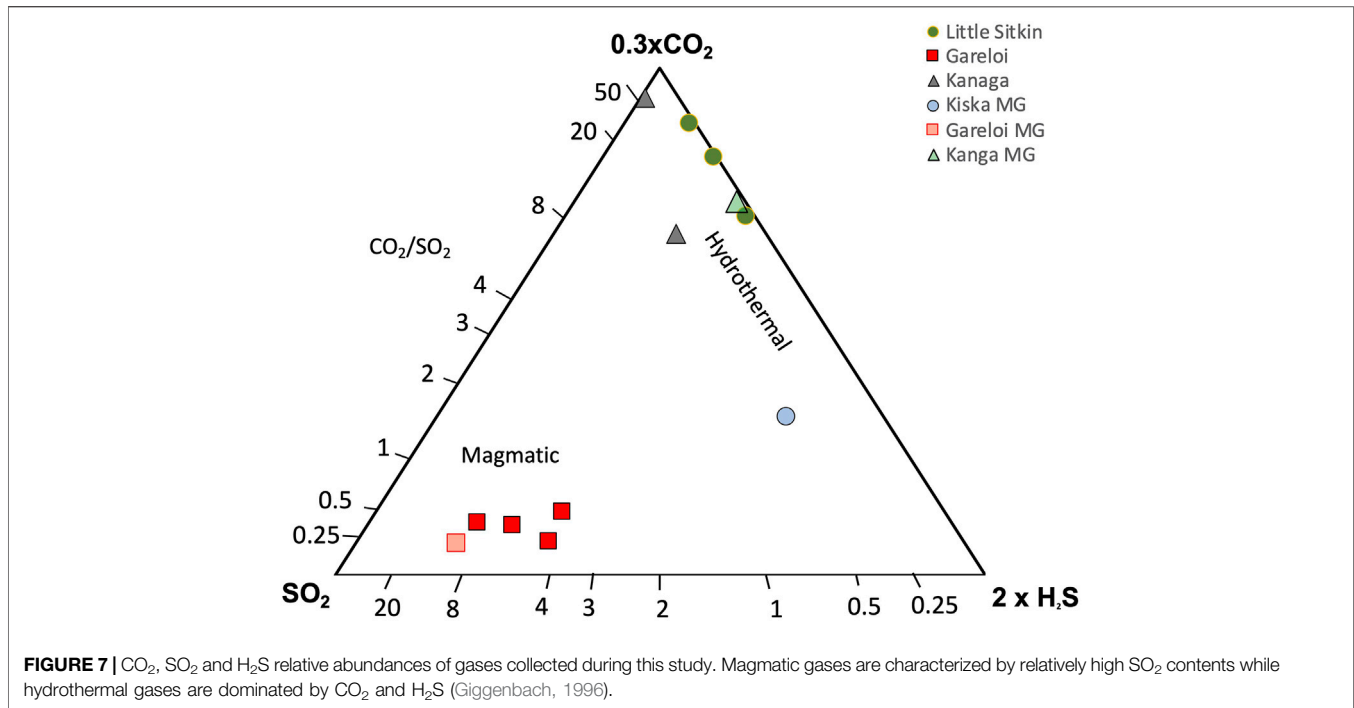
At Kanaga wind speed of 12 m/s was measured and the SO<sub>2</sub> flux calculated by averaging 7 helicopter traverses was 70 ± 30 tons SO<sub>2</sub>/day. At Kiska the average flux of two walking traverses was only 3.6 ± 0.1 tons SO<sub>2</sub>/day, using a measured wind speed of 4.6 m/s. For Gareloi, we use the wind speed of 13.6 m/s to obtain a SO<sub>2</sub> emission rate of 320 ± 80 tons SO<sub>2</sub>/day, averaged over 5 helicopter traverses. This was the highest average flux observed during our field campaign. The flight path of the helicopter and obtained SO<sub>2</sub> burdens are shown in **Figure 5**.

## DISCUSSION

### Major Gases

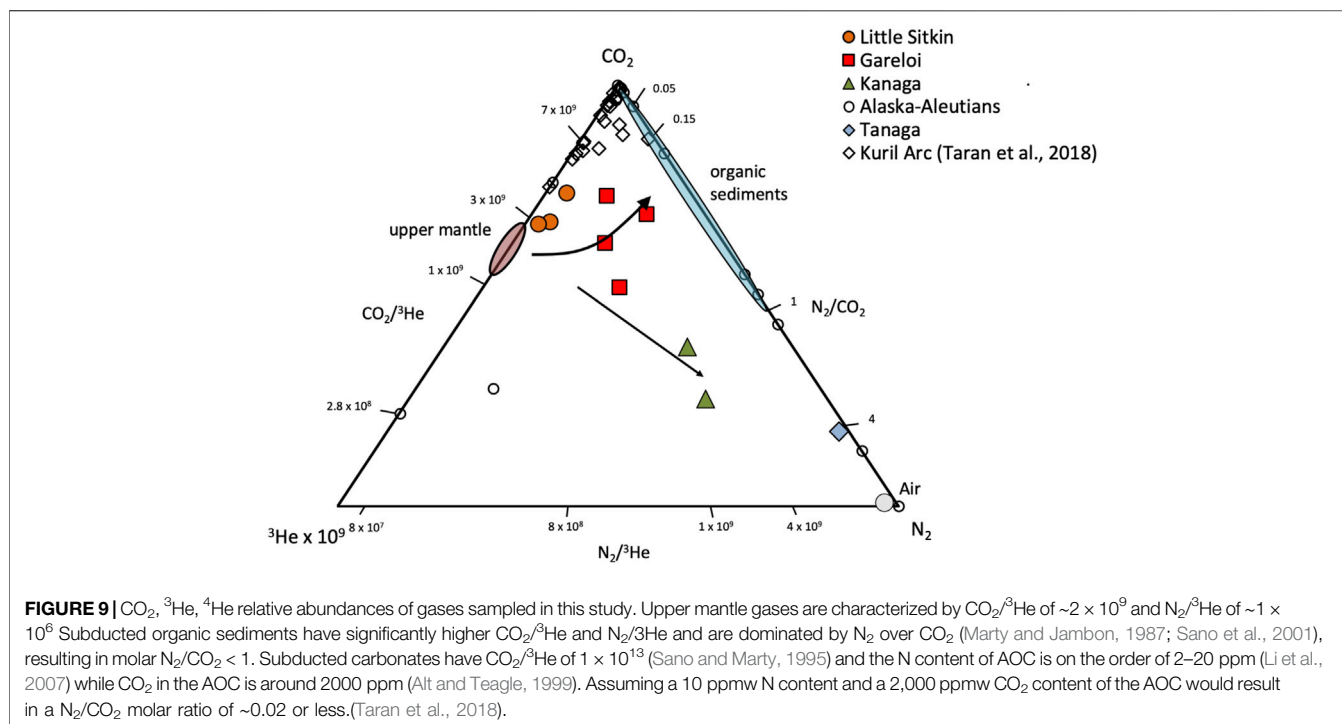
The compositions of the major gases are shown in **Figure 6**, along with a compilation of high-temperature arc gases from the literature (Henley and Fischer, 2021; Taran and Zelenski, 2015). Notably, the ratios obtained by the Multi-GAS are within the range of gas compositions obtained by direct fumarole sampling, supporting the notion that the two measurement and sampling approaches are complementary and can be used interchangeably depending on which approach is more feasible in a given situation. At Gareloi (270°C) the CO<sub>2</sub>/S<sub>t</sub> ratio between the four collected samples ranges from 0.3–0.6 while the H<sub>2</sub>O/S<sub>t</sub> ratio of three direct gas samples ranges from 97 to 137, with the fourth sample being an

outlier with much lower H<sub>2</sub>O/S<sub>t</sub> ratio of 35. Given that the Multi-GAS recorded a H<sub>2</sub>O/S<sub>t</sub> ratio of 75, we attribute the low H<sub>2</sub>O/S<sub>t</sub> ratio of sample 2bS29 to water loss during sampling, consistent with significantly lower water contents of that sample compared to the three others (953 mmol/mol vs 983 mmol/mol). The low CO<sub>2</sub>/SO<sub>2</sub> ratio signature is consistent with that previously proposed for the Aleutian-Kamchatka Pacific arc segment indicating relatively low slab-derived carbon contribution to gas discharges compared to other arcs (Aiuppa et al., 2017; Aiuppa et al., 2019). Low CO<sub>2</sub>/S<sub>t</sub> ratios may also indicate an extensively degassed magma that has lost most of its CO<sub>2</sub> compared to S (Giggenbach, 1996). The low temperature (~boiling point) samples from Kiska, Kanaga, and Little Sitkin display significantly higher CO<sub>2</sub> contents and CO<sub>2</sub>/S<sub>t</sub> ratios in excess of 4 with most samples' CO<sub>2</sub>/S<sub>t</sub> > 8. Little Sitkin gases are typical low temperature hydrothermal gases dominated by H<sub>2</sub>O and CO<sub>2</sub>. In terms of their H<sub>2</sub>O/S<sub>t</sub> ratios, Little Sitkin, Kiska, and Gareloi fall within 40–150, a typical range for arc gases. Notably, the Multi-GAS data set collected for Little Sitkin has a higher H<sub>2</sub>O/S<sub>t</sub> (~1,000) compared to the gas samples (~50). This is likely due to the high and variable humidity at Little Sitkin fumarole and spring area that may have compromised the Multi-GAS H<sub>2</sub>O measurements, as suggested by the low R<sup>2</sup> value (**Figure 3**). Kanaga gases have the highest H<sub>2</sub>O/S<sub>t</sub> ratios of all the gases sampled or measured, likely due to the addition of significant meteoric water in the subsurface. The sample collected at the bubbling spring of Tanaga is dominated by H<sub>2</sub>O. Gareloi and Kiska gas compositions lie in the typical range of high temperature arc gases, even though they have significantly lower outlet temperatures (although we were not able to measure Kiska temperature), suggesting that these volcanic



gases have had minimal interaction with hydrothermal systems (Giggenbach, 1996). This notion is also supported by data presented in **Figure 7** that show the highest  $\text{SO}_2/\text{H}_2\text{S}$  ratios for Gareloi, indicating a stronger magmatic gas signature, and significantly lower  $\text{SO}_2/\text{H}_2\text{S}$  for Little Sitkin and Kanaga, indicating mixed magmatic-hydrothermal signatures. Multi-GAS data from Kiska shows significantly lower  $\text{SO}_2/\text{H}_2\text{S}$  than Gareloi but overall higher sulfur contents than the two volcanoes

dominated by hydrothermal gas discharges (Little Sitkin and Kanaga). In summary, there is good agreement between data collected by Multi-GAS and by direct gas sampling of fumaroles irrespective of gas outlet temperature or magmatic/hydrothermal character of the gases. Gareloi and Kiska have the most magmatic major gas compositions of the Western Aleutians volcanoes investigated and their compositions overlap with global high temperature arc gases from the literature.

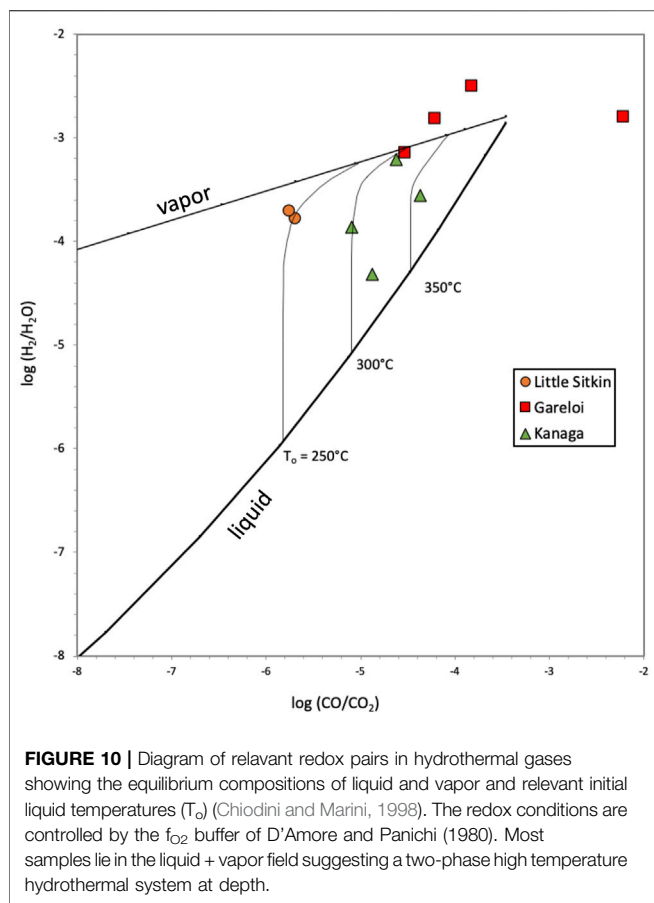


## Minor Gases and Redox Pairs

Trace gas  $\text{N}_2$ , He, and Ar of Western Aleutian samples are shown in **Figure 8** along with data from gas samples collected at other Alaska-Aleutian volcanoes (Evans et al., 2015; Symonds et al., 2003a) and from the geographically similar Kuril Island Arc (Taran et al., 2018). Our data display a range in compositions typical of arc gases world-wide (Giggenbach, 1996) with  $\text{N}_2/\text{He}$  ratios generally  $>1,000$  and He/Ar ratios affected by variable amounts of mixing with air or air-saturated water. Gases from Little Sitkin show the lowest  $\text{N}_2/\text{He}$  ratios with samples from both the fumarole and bubbling spring plotting at values close to or below the typical arc-type range. We note that the definition of the arc-type field with  $\text{N}_2/\text{He}$  values from 1,000–10,000 by Giggenbach (1996) was based on significantly fewer data available at the time. More recent additions of data from samples collected from gas discharges of volcanoes in oceanic arc settings (Kuril Islands (Taran et al., 2018), Izu Bonin Marianas (Mitchell et al., 2010), Sangihe (Clor et al., 2005)) display  $\text{N}_2/\text{He}$  values at the lower end of this range, in the mantle field or in some cases between these endmembers. The upper mantle-like  ${}^3\text{He}/{}^4\text{He}$  values (7.0–8.3 Ra) that preclude significant crustal contamination of the gases and the higher than mantle  $\text{N}_2/\text{He}$  ratios are indicative of  $\text{N}_2$  addition from the subducted slab. Recent thermochemical modeling work by Epstein et al. (2021) in the Hikurangi margin suggests that N generally is better retained than C during subduction an observation that may explain some of the lower  $\text{N}_2/\text{He}$  ratios in some arcs and supports the idea of subduction of some of the N past the zone of arc magma generation (Busigny et al., 2003; Mitchell et al., 2010). The Western Aleutians data also overlap with the Kuril Islands data; however, some of the Kuril volcanoes

indicate a more dominant mantle source for  $\text{N}_2$ , i.e. low  $\text{N}_2/\text{He}$  at high He/Ar values, displacing them close to the mantle gas field (**Figure 8**). Like the Western Aleutians gases, the Kuril  ${}^3\text{He}/{}^4\text{He}$  values of the least air contaminated samples have air-corrected values ranging between 7.0 and 8.3 Ra (Taran et al., 2018). This consistency in  ${}^3\text{He}/{}^4\text{He}$  ratios between these two oceanic arcs implies that oceanic arc gases are generally less affected than those from continental arcs by contributions of volatiles from crustal sources (Sano and Fischer, 2013), providing the opportunity to investigate slab-derived volatile sources.

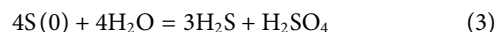
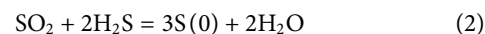
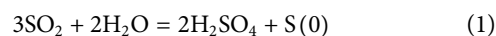
**Figure 9** shows relative abundances of  ${}^3\text{He}$ ,  $\text{N}_2$  and  $\text{CO}_2$ . The upper mantle has  $\text{CO}_2/{}^3\text{He}$  of  $\sim 2 \times 10^9$  and  $\text{N}_2/{}^3\text{He}$  of  $\sim 1 \times 10^6$ . Subducted organic sediments have significantly higher  $\text{CO}_2/{}^3\text{He}$  ( $1 \times 10^{13}$ ) and  $\text{N}_2/{}^3\text{He}$  ( $1 \times 10^{12}$ ) (Marty and Jambon, 1987; Sano and Marty, 1995; Sano et al., 2001), resulting in molar  $\text{N}_2/\text{CO}_2 < 1$ . Subducted carbonates sourced either from the altered oceanic crust (AOC) or sedimentary carbonates have  $\text{CO}_2/{}^3\text{He}$  of  $1 \times 10^{13}$  (Sano and Marty, 1995). As the Aleutians are located in northern latitudes, there is minimal subducted sedimentary carbonate delivered to the trench (Plank and Langmuir, 1998) and it can be ruled out as contributing significantly to volcanic gas discharges, leaving the AOC as the only potential source of carbonate-derived carbon to Aleutian gas discharges. The N content of AOC is generally assumed to be quite low, on the order of 2–20 ppm (Li et al., 2007) while  $\text{CO}_2$  in the AOC is around 2,000 ppm (Alt and Teagle, 1999). Assumption of a 10 ppmw N content and a 2000 ppmw  $\text{CO}_2$  content for the AOC would result in a molar  $\text{N}_2/\text{CO}_2$  ratio of  $\sim 0.02$  or less, overlapping with the lower end of the organic sediment field in **Figure 9**. The diagram illustrates that gases from Little Sitkin lie closest to the mantle endmember, with a composition reflecting a



mixture of predominantly mantle and AOC sources. Gases from Gareloi have the most organic sedimentary  $\pm$  AOC contributions, based on their relatively high  $N_2/{}^3\text{He}$  and high  $N_2/\text{CO}_2$ , while gases from Kanaga and Tanaga can be explained by a predominantly mantle source mixing with air. It is also apparent that gases from Little Sitkin and Gareloi have  $\text{CO}_2/{}^3\text{He}$  ratios that overlap with or are only slightly higher than the mantle endmember, indicating that slab-derived carbon addition in this part of the arc is likely minor. However, we note that samples from Gareloi display  $N_2$ -He-Ar relative abundances (Figure 8) that indicate significant air contamination and therefore,  $N_2$  and  $\text{CO}_2$  sources need to be treated with caution. Samples from Kanaga and Tanaga are also displaced towards the air component in Figure 8, compromising any evaluation of deep source contributions of  $N_2$  to these gas discharges. Our samples from the Western Aleutians generally display lower  $\text{CO}_2/{}^3\text{He}$  ratios than the samples from the Kuril arc (Taran et al., 2018), suggesting that gases in the Western Aleutians have a lower slab  $\text{CO}_2$  contribution than gases from the Kuril Islands. Lopez et al (in prep) utilize C-isotopes to investigate in detail the contribution of slab derived carbon and how it varies along the Aleutian Arc, and find predominantly mantle and/or AOC carbon sources in the Western Aleutians.

Figure 10 shows that for commonly used redox pairs for  $\text{H}_2/\text{H}_2\text{O}$  and  $\text{CO}/\text{CO}_2$  (Chiodini and Marini, 1998) and using the

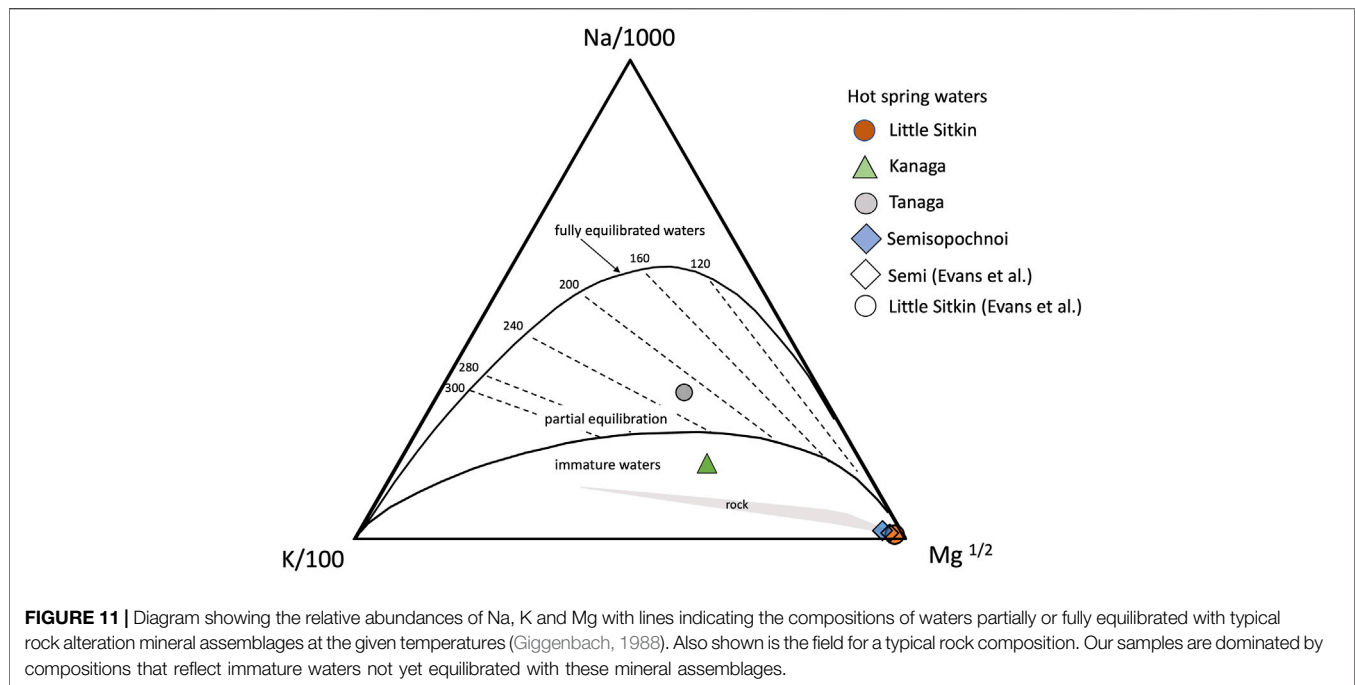
buffer system of D'Amore and Panichi (1980), the samples for which CO was detected (Kanaga and Gareloi) would have equilibrium temperatures of around 350°C. We note, however, that both Kanaga and Gareloi gas compositions are widely dispersed on this diagram making this assessment qualitative only. If correct, the high equilibrium temperatures in the liquid plus vapor field for Kanaga are consistent with the comparatively high  $\text{CO}_2/S_t$  and low  $\text{SO}_2/\text{H}_2\text{S}$  ratios (Figures 6, 7) that suggest S deposition at depth and production of  $\text{H}_2\text{S}$  according to the following from (Giggenbach, 1996):



Therefore, Kanaga likely remains a highly active volcano with a high temperature magmatic-hydrothermal system just below the surface, although  $\text{SO}_2$  degassing levels are low ( $70 \pm 30$  t  $\text{SO}_2/\text{day}$ ) and fumaroles are diffuse. For Gareloi, one sample (1a S1) has unusually high CO contents, compared to the duplicate sample (1b S14) and the other samples from Gareloi that were collected at higher temperature sites (2a and 2b), resulting in unrealistically high  $\log(\text{CO}/\text{CO}_2)$  values of  $-2.2$ . We assume that this is likely due to an analytical issue. All other Gareloi samples lie within the vapor field at high temperatures ( $>350^\circ\text{C}$ ) consistent with the magmatic character of these fumarole gases. Unfortunately, the inaccessibility of the Kiska fumarole precluded adequate collection of gas samples, making an evaluation of the equilibrium temperatures impossible. However, the extensive deposition of native sulfur around the vent area (Figure 2A) strongly suggests reactions of  $\text{SO}_2$  according to 1) and 2) implying that Kiska also hosts pressurized magmatic-hydrothermal system, which is emitting roaring gases at the one fumarole. We also plotted the data for the Little Sitkin fumarole gas using the detection limit for CO (0.0002 mmol/mol), and the resulting minimum equilibrium temperatures are 250°C in a mixed liquid + vapor phase. We note that CO contents of Little Sitkin gases could be lower resulting in temperatures below 250°C. Therefore, quantitative assessment of Little Sitkin deep temperatures is not possible with these data.

## Thermal Waters

Thermal water from the Western Aleutians are shown in the classic plot of Giggenbach (1988) in Figure 11 with the theoretical lines representing equilibrium compositions with a typical hydrothermal mineral composition including K- and Na feldspars, micas and chloride. The intersection of each isotherm with the full equilibrium line indicates that the waters are in full equilibrium with this mineral assemblage at the indicated temperature. Displacement towards the Mg-rich corner of the diagram indicates that the sampled waters are either mixtures of hydrothermal fluids with shallow ground-waters or that the reactions involving Mg have quickly equilibrated during ascent of the thermal waters to the surface (i.e. Chiodini et al. (2015)). In both instances, as long as the waters lie between the fully and partially equilibrated curves, the Na-Mg and Na-K



geothermometers still provide a valid estimate of the hydrothermal temperatures. The Mg-rich waters of Semisopochnoi and Little Sitkin lie close to the Mg-apex and overlap with the typical rock composition, indicating that these waters are immature waters and have not equilibrated with the alteration mineral assemblage. The Kanaga water sample approaches the partial equilibrium line but its composition also suggests immature water composition, out of equilibrium with relevant alteration mineral assemblages. Only Tanaga has a composition that lies in the field of partially equilibrated waters. Its Na-Mg temperature is around 220°C, consistent with a high temperature hydrothermal system at depth. Tanaga water temperature was measured at 62°C but no fumaroles were available for gas sampling to evaluate deep temperatures using gas geothermometry.

## SO<sub>2</sub> and CO<sub>2</sub> Fluxes

SO<sub>2</sub> fluxes from Western Aleutian volcanoes are 3.6 ± 0.1 t/day (Kiska), 70 ± 30 t/day (Kanaga) and 320 ± 80 t/day (Gareloi) and are typical of the low to moderate fluxes similar to many passively degassing arc volcanoes (Shinohara, 2013; Carn et al., 2017; Fischer et al., 2019; Werner et al., 2019). CO<sub>2</sub> fluxes can be estimated by combining the CO<sub>2</sub>/SO<sub>2</sub> ratios of direct gas emissions with measured SO<sub>2</sub> fluxes (Fischer et al., 1998; Aiuppa et al., 2019; Fischer et al., 2019). While this common approach provides reasonable estimates, it has been pointed out that crater plume or fumarole C/S ratios may not always be representative of the overall C/S ratios in the plume, especially if not measured at the same time as SO<sub>2</sub> flux, and may lead to erroneous CO<sub>2</sub> fluxes (Burton et al., 2013). These authors argue that direct airborne measurements of CO<sub>2</sub> in the plume and contemporaneous C/S ratio measurements improve the accuracy of the CO<sub>2</sub> estimates. Recently Fischer and Aiuppa (2020) showed

that high-temperature fumarole compositions and multi-GAS measurements obtained from crater plumes combined with ground-based or satellite-based SO<sub>2</sub> emission provide robust CO<sub>2</sub> fluxes for volcanoes where degassing is dominated by crater emissions. However, estimating the CO<sub>2</sub> fluxes of volcanoes that have SO<sub>2</sub> emissions that are not detectable by satellite, and therefore are likely dominated by hydrothermal and diffuse emissions rich in H<sub>2</sub>S and CO<sub>2</sub>, provides a significant challenge in estimating a global CO<sub>2</sub> flux that also includes low emitters (Fischer et al., 2019; Werner et al., 2019; Fischer and Aiuppa, 2020). Due to constraints on time and access, we were unable to measure diffuse CO<sub>2</sub> emissions by accumulation chamber (Chiodini et al., 1998) and we did not have the necessary instrumentation to measure CO<sub>2</sub> concentrations in the plume by airborne techniques (Werner et al., 2009). However, our data from direct fumarole samples and from crater plume multi-GAS measurements enable the estimation of CO<sub>2</sub> flux from these volcanoes while addressing some of the issues mentioned above. For Gareloi, the high temperature (270°C) fumarole and multi-GAS CO<sub>2</sub>/SO<sub>2</sub> and CO<sub>2</sub>/S<sub>t</sub> ratios agree well (Table 4). The direct fumarole samples have a CO<sub>2</sub>/S<sub>t</sub> of 0.41 ± 0.11 while the Multi-GAS shows 0.20 for that same ratio. The Multi-GAS CO<sub>2</sub>/SO<sub>2</sub> ratio (0.26) is essentially identical to that CO<sub>2</sub>/S<sub>t</sub> ratio (0.20) and the direct samples' CO<sub>2</sub>/SO<sub>2</sub> and CO<sub>2</sub>/S<sub>t</sub> ratios (0.34–0.69 and 0.28 to 0.55, respectively) due to the predominance of SO<sub>2</sub> as the S species degassing from high T fumaroles. Using these ratios, we obtain a CO<sub>2</sub> flux from Gareloi of 1.17 × 10<sup>4</sup> mol C/yr or 5.14 × 10<sup>5</sup> g/yr (5.14 ± 1.3 × 10<sup>-7</sup> Tg/yr). Similarly for Kiska, where we observed degassing from one massive fumarole, the CO<sub>2</sub>/S<sub>t</sub> and CO<sub>2</sub>/SO<sub>2</sub> ratios obtained by Multi-GAS are within a factor of two (2.5 and 5.09, respectively). Using this ratio, the CO<sub>2</sub> flux from Kiska is 3,090 ± 1,445 mol/yr or 1.3 ± 0.6 × 10<sup>-7</sup> Tg/yr.

For Kanaga, the Multi-GAS  $\text{CO}_2/\text{S}_t$  ratios and  $\text{CO}_2/\text{SO}_2$  ratios differ significantly (18 and 186, respectively). Likewise,  $\text{CO}_2/\text{S}_t$  and  $\text{CO}_2/\text{SO}_2$  ratios from direct samples differ significantly and differ between gases collected from different fumaroles. At Kanaga,  $\text{H}_2\text{S}$  is a significant sulfur species and ten times more abundant than  $\text{SO}_2$  as measured by Multi-GAS. Notably, the direct samples have variable  $\text{H}_2\text{S}$  contents, likely due to the low overall S concentrations in the gas, making  $\text{SO}_2$  versus  $\text{H}_2\text{S}$  distinction challenging using our wet-chemistry based analytical methods. We therefore consider the Multi-GAS  $\text{CO}_2/\text{SO}_2$  and  $\text{CO}_2/\text{H}_2\text{S}$  ratios more reliable. While it has been shown that  $\text{H}_2\text{S}$  will readily oxidize to  $\text{SO}_2$  during high temperature (1,000 °C) mixing of magmatic gases with the atmosphere (Martin et al., 2006), low temperature oxidation is likely to be much slower. Because Kanaga equilibrium temperatures are ~300 °C and outlet temperatures are only boiling, extensive high temperature oxidation of  $\text{H}_2\text{S}$  to  $\text{SO}_2$  is unlikely and we therefore use the Multi-GAS  $\text{CO}_2/\text{SO}_2$  ratio for our flux estimate. This approach results in a Kanaga  $\text{CO}_2$  flux of  $2.38 \times 10^6$  mol/yr or  $1.05 \pm 0.45 \times 10^{-4}$  Tg/yr. Our data show that while Gareloi is the largest  $\text{SO}_2$  emitter of the Western Aleutians, Kanaga is the largest  $\text{CO}_2$  emitter. Our data do not include any diffuse degassing or any flank degassing, only crater degassing.

The volcanoes of the Western Aleutians emit about  $1 \pm 0.4 \times 10^{-4}$  Tg  $\text{CO}_2$ /yr, a small fraction of the 1.66 Tg  $\text{CO}_2$  (taking into account extrapolations of non-measured volcanoes) emitted by the entire Alaska-Aleutian volcanic arc (Fischer et al., 2019). Using these workers' data, it is interesting to note that the volcanic  $\text{CO}_2$  emissions increase significantly from the Western Aleutians ( $0.0001$  Tg $\text{CO}_2$ /yr) to the Central ( $0.1 \pm 0.09$  Tg $\text{CO}_2$ /yr) and Eastern Aleutians ( $0.12 \pm 0.08$  Tg $\text{CO}_2$ /yr) and to the Alaska Peninsula ( $1.03 \pm 0.48$  Tg $\text{CO}_2$ /yr). When we normalize these fluxes by approximate arc segment lengths (Western Arc 500 km, Central Arc 750 km, Eastern Arc 1,100 km, **Figure 1**), we notice orders of magnitude changes in  $\text{CO}_2$  fluxes per km with the Western Arc emitting only  $2.2 \times 10^{-7}$  Tg $\text{CO}_2$ /yr/km, the Central Arc emitting  $1.3 \times 10^{-4}$  Tg $\text{CO}_2$ /yr/km and the Eastern Arc emitting  $1.05 \times 10^{-3}$  Tg $\text{CO}_2$ /yr/km. The above values take into account only the volcanoes that have been measured and reported in Fischer et al. (2019). Applying these authors' extrapolation method, to include not measured volcanoes does not significantly change these fluxes for the eastern and central segments ( $1.13 \times 10^{-3}$  Tg $\text{CO}_2$ /yr/km for eastern,  $1.46 \times 10^{-4}$  Tg $\text{CO}_2$ /yr/km for central) but increases the flux of the western segment to  $1.04 \times 10^{-4}$  Tg $\text{CO}_2$ /yr/km. The remote western segment has four volcanoes that are hydrothermally active (Great Sitkin, Moffet, Tanaga and Little Sitkin) but have not been measured for  $\text{CO}_2$  emissions. As these volcanoes have been ascribed a flux of 0.013 Tg $\text{CO}_2$ /yr each in (Fischer et al., 2019), this extrapolated flux of 0.052 Tg $\text{CO}_2$ /yr is larger than what we measured for all western Aleutian volcanoes combined ( $0.001$  Tg $\text{CO}_2$ /yr/km), leading to a significantly higher estimated flux. Future studies should focus on measuring  $\text{CO}_2$  fluxes from these volcanoes.

Plate convergence is near orthogonal in the eastern and central portion of the arc and gradually becomes more oblique in the western region of the Aleutian Arc, with plate motion eventually

transitioning to strike-slip near ~170°E (**Figure 1**) (DeMets et al., 1990; Buurman et al., 2014). The varying convergence angles, combined with the thickness of subducted sediment, result in highly variable subducted sediment fluxes along the length of the arc, with a maximum in the central Aleutians and a minimum in the western Aleutians (Kelemen et al., 2003). The Eastern Aleutians are characterized by thicker continental crust (Flügel and Klempner, 2000). These along-strike variations in subduction parameters and crustal thickness may potentially affect the observed volcanic  $\text{CO}_2$  output along the strike of the arc as is discussed in more detail in (Lopez et al., in preparation).

## CONCLUSION

Our new data of gas and spring discharges from the Western Aleutian volcanoes provide key information about the nature of the volcano-hydrothermal systems in this region. The results indicate that all the volcanoes investigated host high-temperature mixed liquid-vapor systems that are fed by volatiles primarily sourced from the mantle wedge and the subducted slab, with negligible crustal contamination. In particular, Kiska, Kanaga and Gareloi have gas compositions that indicate a significant magmatic degassing component. Our measured  $\text{SO}_2$  and  $\text{CO}_2$  fluxes provide background values during a low-level of activity that provide a baseline against which future fluxes can be compared and evaluated in light of changes in volcanic activity. The Aleutian Arc is well known for its along-strike variations in subduction parameters such as convergence angle, amount of sediment delivery to the trench and crustal thickness. While more work on volcanic gas fluxes is needed, especially in the remote regions of the arc, our data suggests that volcanic  $\text{CO}_2$  fluxes are lowest where convergence angle is most oblique and sediment delivery to the trench is at its minimum.

## DATA AVAILABILITY STATEMENT

The original contributions presented in the study are included in the article/**Supplementary Material**, further inquiries can be directed to the corresponding author.

## AUTHOR CONTRIBUTIONS

TF helped obtain the funding, collected most of the samples and data, coordinated the analyses, made most of the figures and wrote the article. TL helped obtain the funding collected some of the samples and data, performed most of the analyses and contributed to the article. AA provided instrumentation to make some of the measurements, plotted some of the data and contributed to the article AR analyzed some of the samples and contributed to the article TI analyzed some of the samples and contributed to the article KK obtained funding, was co-Scientist in Charge of the cruise and contributed to the article EC obtained funding, was co-Scientist in Charge of the cruise, provided a figure and contributed to the article.

## FUNDING

This work was funded by NSF EAR GeoPRISMS 1347248 to EC, a Smithsonian Scholarly Studies Grant to EC, NSF EAR GeoPRISMS 1347330 to KK, by NSF GeoPRISMS grant 1551978 to TF and TL and by support from the Deep Carbon Observatory-DECADE Initiative to TF and TL.

## ACKNOWLEDGMENTS

We thank the individuals and organizations that made the summer field season of 2015 possible aboard the third leg of the NSF GeoPRISMS shared platform for Aleutians research, including Captain Raines and the crew of the R/V Maritime Maid, pilot Dan Leary and Maritime Helicopters, Christie Hauptert at Polar Field Services, EAR NSF program officers,

the USGS Natural Hazards Program, the Deep Carbon Observatory, DECADE Initiative, and the shipboard scientific party. We thank Michelle Coombs for comments on the manuscript and Samantha Wolf for help with the figures. We thank Viorel Atudorei, UNM Center for Stable isotopes for help with nitrogen isotope measurements. We thank Antonio Paonita for handling this manuscript as editor and two reviewers for comments on an earlier version of this manuscript.

## SUPPLEMENTARY MATERIAL

The Supplementary Material for this article can be found online at: <https://www.frontiersin.org/articles/10.3389/feart.2021.786021/full#supplementary-material>

## REFERENCES

- Aiuppa, A., Fischer, T. P., Plank, T., and Bani, P. (2019). CO<sub>2</sub> Flux Emissions from the Earth's Most Actively Degassing Volcanoes, 2005-2015. *Sci. Rep.* 9, 5442. doi:10.1038/s41598-019-41901-y
- Aiuppa, A., Frederico, C., Giudice, G., and Gurrieri, S. (2005). Chemical Mapping of a Fumarolic Field: La Fossa Crater, Vulcano Island (Aeolian Islands, Italy). *Geophys. Res. Lett.* 32, L13309. doi:10.1029/2005GL023207
- Aiuppa, A., Robidoux, P., Tamburello, G., Conde, V., Galle, B., Avarod, G., et al. (2014). Gas Measurements from the Costa Rica-Nicaragua Volcanic Segment Suggest Possible Along-Arc Variations in Volcanic Gas Chemistry. *Earth Planet. Sci. Lett.* 407, 134-147. doi:10.1016/j.epsl.2014.09.041
- Alt, J. C., and Teagle, D. A. H. (1999). The Uptake of Carbon during Alteration of Ocean Crust. *Geochimica et Cosmochimica Acta* 63, 1527-1535. doi:10.1016/s0016-7037(99)00123-4
- Battaglia, A., Bitetto, M., Aiuppa, A., Rizzo, A. L., Chigna, G., Watson, I. M., et al. (2018). The Magmatic Gas Signature of Pacaya Volcano, with Implications for the Volcanic CO<sub>2</sub> Flux from Guatemala. *Geochem. Geophys. Geosystems* 19, 667-692. doi:10.1002/2017gc007238
- Bergfeld, D., Lewicki, J. L., Evans, W. C., Hunt, A. G., Revesz, K., and Huebner, M. (2013). Geochemical Investigation of the Hydrothermal System on Akutan Island, Alaska. U.S. Geological Survey Scientific Investigation Report 2013-5231. Reston, Virginia: U.S. Geological Survey, 1-19.
- Burton, M. R., Sawyer, G. M., and Granieri, D. (2013). Deep Carbon Emissions from Volcanoes. *Rev. Mineralogy Geochem.* 75, 323-354. doi:10.2138/rmg.2013.75.11
- Busigny, V., Cartigny, P., Philippot, P., Ader, M., and Javoy, M. (2003). Massive Recycling of Nitrogen and Other Fluid-mobile Elements (K, Rb, Cs, H) in a Cold Slab Environment: Evidence from HP to UHP Oceanic Metasediments of the Schistes Lustrés Nappe (Western Alps, Europe). *Earth Planet. Sci. Lett.* 215, 27-42. doi:10.1016/S0012-821X(03)00453-9
- Buurman, H., Nye, C. J., West, M. E., and Cameron, C. (2014). Regional Controls on Volcano Seismicity along the Aleutian Arc. *Geochem. Geophys. Geosyst.* 15, 1147-1163. doi:10.1002/2013gc005101
- Cameron, C. E., Schaefer, J. R., and Ekberg, P. G. (2020). Historically Active Volcanoes of Alaska. Alaska Division of Geological & Geophysical Surveys Miscellaneous Publication 133 v. 4, 2 sheets.
- Carn, S. A., Fioletov, V. E., McLinden, C. A., Li, C., and Krotkov, N. A. (2017). A Decade of Global Volcanic SO<sub>2</sub> Emissions Measured from Space. *Sci. Rep.* 7, 44095. doi:10.1038/srep44095
- Casadevall, T. J., Doukas, M. P., Neal, C. A., McGimsey, R. G., and Gardner, C. A. (1994). Emission Rates of Sulfur Dioxide and Carbon Dioxide from Redoubt Volcano, Alaska during the 1989-1990 Eruptions. *J. Volcanology Geothermal Res.* 62, 519-530. doi:10.1016/0377-0273(94)90050-7
- Chiodini, G., Cioni, R., Guidi, M., Raco, B., and Marini, L. (1998). Soil CO<sub>2</sub> Flux Measurements in Volcanic and Geothermal Areas. *Appl. Geochem.* 13 (5), 543-552. doi:10.1016/s0883-2927(97)00076-0
- Chiodini, G., Liccioli, C., Vaselli, O., Calabrese, S., Tassi, F., Caliro, S., et al. (2015). The Domuyo Volcanic System: An Enormous Geothermal Resource in Argentine Patagonia. *J. Volcanol. Geotherm. Res.* 274, 71-77. doi:10.1016/j.jvolgeores.2014.02.006
- Chiodini, G., and Marini, L. (1998). Hydrothermal Gas Equilibria: the H<sub>2</sub>O-H<sub>2</sub>-CO<sub>2</sub>-CO-CH<sub>4</sub> System. *Geochim. Cosmochim. Acta* 62, 2673e2687. doi:10.1016/s0016-7037(98)00181-1
- Clor, L. E., Fischer, T. P., Hilton, D. R., Sharp, Z. D., and Hartono, U. (2005). Volatile and N Isotope Chemistry of the Molucca Sea Collision Zone: Tracing Source Components along the Sangihe Arc, Indonesia. *Geochem. Geophys. Geosyst.* 6, a-n. doi:10.1029/2004GC000825
- Coombs, M. L., McGimsey, R. G., and Browne, B. L. (2008). Preliminary Volcano-hazard Assessment for Gareloi Volcano, Gareloi Island, Alaska. *U.S. Geol. Surv. Scientific Invest. Rep.* 2008-5159, 26. doi:10.3133/sir20085159
- Coombs, M. L., McGimsey, R. G., and Browne, B. L. (2007). Preliminary Volcano-hazard Assessment for the Tanaga Volcanic Cluster, Tanaga Island, Alaska. *U.S. Geol. Surv. Scientific Invest. Rep.* 2007-5094, 36, 2007. Available at: <http://pubs.usgs.gov/sir/2007/5094/>.
- de Moor, J. M., Fischer, T. P., Sharp, Z. D., Hilton, D. R., Barry, P. H., Mangasini, F., et al. (2013a). Gas Chemistry and Nitrogen Isotope Compositions of Cold Mantle Gases from Rungwe Volcanic Province, Southern Tanzania. *Chem. Geology* 339, 30-42. doi:10.1016/j.chemgeo.2012.08.004
- de Moor, J. M., Fischer, T. P., Sharp, Z. D., King, P. L., Wilke, M., Botcharnikov, R. E., et al. (2013b). Sulfur Degassing at Erta Ale (Ethiopia) and Masaya (Nicaragua) Volcanoes: Implications for Degassing Processes and Oxygen Fugacities of Basaltic Systems. *Geochem. Geophys. Geosyst.* 14, 4076-4108. doi:10.1002/ggge.20255
- DeMets, C., Gordon, R. G., Argus, D. F., and Stein, S. (1990). Current Plate Motions. *Geophys. J. Int.* 101, 425-478. doi:10.1111/j.1365-246x.1990.tb06579.x
- Doukas, M., and McGee, K. (2007). A Compilation of Gas Emission-Rate Data from Volcanoes of Cook Inlet (Spurr, Crater Peak, Redoubt, Iliamna, and Augustine) and Alaska Peninsula (Douglas, Fourpeaked, Griggs, Mageik, Martin, Peulik, Ukinrek Maars, and Veniaminof), Alaska, from 1995-2006. Open-File Report 02-395. Reston, Virginia: U.S. Geological Survey.
- Doukas, M. P. (1995). A Compilation of Sulfur Dioxide and Carbon Dioxide Emission-Rate Data from Cook Inlet Volcanoes (Redoubt, Spurr, Iliamna, and Augustine), Alaska during the Period from 1990-1994. USGS Open-File Report, 95-55. Reston, Virginia: U.S. Geological Survey.
- Doukas, M. P. (2002). A New Method for GPS-Based Wind Speed Determinations during Airborne Volcanic Plume Measurements. USGS Open-File Report 02-395. Reston, Virginia: U.S. Geological Survey.
- Epstein, G. S., Bebout, G. E., Christenson, B. W., Sumino, H., Wada, I., Werner, C., et al. (2021). Cycling of CO<sub>2</sub> and N<sub>2</sub> along the Hikurangi Subduction Margin,

- New Zealand: An Integrated Geological, Theoretical, and Isotopic Approach. *Geochem. Geophys. Geosys.* 22, e2021GC009650. doi:10.1029/2021GC009650
- Evans, W. C., Bergfeld, D., McGimsey, R. G., and Hunt, A. G. (2009). Diffuse Gas Emissions at the Ukinrek Maars, Alaska: Implications for Magmatic Degassing and Volcanic Monitoring. *Appl. Geochem.* 24, 527–535. doi:10.1016/j.apgeochem.2008.12.007
- Evans, W. C., Bergfeld, D., Neal, C. A., McGimsey, R. G., Werner, C. A., Waythomas, C. F., et al. (2015). Aleutian Arc Geothermal Fluids: Chemical Analyses of Waters and Gases Sampled in Association with the Alaska Volcano Observatory. *U.S. Geol. Surv. Data Release*. doi:10.5066/F78G8HR1
- Fierstein, J., and Hildreth, W. (1992). The Plinian Eruptions of 1912 at Novarupta, Katmai National Park, Alaska. *Bull. Volcanol* 54 (8), 646–684. doi:10.1007/bf00430778
- Fischer, T. P., and Aiuppa, A. (2020). AGU Centennial Grand Challenge: Volcanoes and Deep Carbon Global CO<sub>2</sub> Emissions from Subaerial Volcanism: Recent Progress and Future Challenges. *G-cubed* 21 (3), e2019GC008690. doi:10.1029/2019gc008690
- Fischer, T. P., Arellano, S., Carn, S., Aiuppa, A., Galle, B., Allard, P., et al. (2019). The Emissions of CO<sub>2</sub> and Other Volatiles from the World's Subaerial Volcanoes. *Sci. Rep.* 9, 18716. doi:10.1038/s41598-019-54682-1
- Fischer, T. P., and Chiodini, G. (2015). Volcanic, Magmatic and Hydrothermal Gases. *Encyclopedia of Volcanoes*. 2nd Edition, 779–797. doi:10.1016/B978-0-12-385938-9.00045-6
- Fischer, T. P., Giggenbach, W. F., Sano, Y., and Williams, S. N. (1998). Fluxes and Sources of Volatiles Discharged from Kudryavy, a Subduction Zone Volcano, Kurile Islands. *Earth Planet. Sci. Lett.* 160, 81–96. doi:10.1016/s0012-821x(98)00086-7
- Fischer, T. P., and Lopez, T. M. (2016). First Airborne Samples of a Volcanic Plume for d<sup>13</sup>C of CO<sub>2</sub> Determinations. *Geophys. Res. Lett.* 43, 3272–3279. doi:10.1002/2016gl068499
- Fliedner, M. M., and Klemperer, S. L. (2000). Crustal Structure Transition from Oceanic Arc to continental Arc, Eastern Aleutian Islands and Alaska Peninsula. *Earth Planet. Sci. Lett.* 179, 567–579. doi:10.1016/s0012-821x(00)00142-4
- Galle, B., Oppenheimer, C., Geyer, A., McGonigle, A. J. S., Edmonds, M., and Horrocks, L. (2002). A Miniaturized Ultraviolet Spectrometer for Remote Sensing of SO<sub>2</sub> Fluxes; a New Tool for Volcano Surveillance. *J. Volcanol. Geotherm. Res.* 119, 241–254. doi:10.1016/S0377-0273(02)00356-6
- Gerlach, T. M., Westrich, H. R., Casadevall, T. J., and Finnegan, D. L. (1994). Vapor Saturation and Accumulation in Magmas of the 1989–1990 Eruption of Redoubt Volcano, Alaska. *J. Volcanology Geothermal Res.* 62, 317–337. doi:10.1016/0377-0273(94)90039-6
- Giggenbach, W. F. (1996). “Chemical Composition of Volcanic Gases,” in *IAVCEI-UNESCO: Monitoring and Mitigation of Volcano Hazards*. Editors R. Scarpa and R. Tilling, 221–256. doi:10.1007/978-3-642-80087-0\_7
- Giggenbach, W. F. (1988). Geothermal Solute Equilibria. Derivation of Na-K-Mg-Ca Geoindicators. *Geochimica et Cosmochimica Acta* 52, 2749–2765. doi:10.1016/0016-7037(88)90143-3
- Giggenbach, W. F., and Goguel, R. L. (1989a). Collection and Analysis of Geothermal and Volcanic Water and Gas Discharges. Report, No. 2401. Department of Scientific and Industrial Research, Chemistry Division.
- Giggenbach, W. F., and Goguel, R. L. (1989b). Methods for the Collection and Analysis of Geothermal and Volcanic Water and Gas Samples. CD 2387. Department of scientific and industrial research, chemistry division.
- Graham, D. W. (2002). “8. Noble Gas Isotope Geochemistry of Mid-ocean Ridge and Ocean Island Basalts: Characterization of Mantle Source Reservoirs,” in *MSA Special Volume: Noble Gases*. Editors D. Porcelli, C. Ballentine, and R. Wieler, 47, 247–318. doi:10.1515/9781501509056-010
- GVP (2013). “Report on Kanaga (United States),” in *Bulletin of the Global Volcanism Network*. Editor R. Wunderman (Washington, DC: Smithsonian Institution), 38, 3. Available at: <https://volcano.si.edu/E3/>. Sep Accessed 25, 2019).
- GVP (2015). “Report on Pavlof (United States),” in *Bulletin of the Global Volcanism Network*. Editor R. Wunderman (Washington, DC: Smithsonian Institution), 40, 4. Available at: <https://volcano.si.edu/E3/>. Sep Accessed 25, 2019).
- GVP (2021a). “Report on Cleveland (United States),” in *Weekly Volcanic Activity Report, 24 March-30 March 2021*. Editor S. K. Sennert (Washington, DC: Smithsonian Institution and US Geological Survey). GVP.WVAR20210324-311240.
- GVP (2021b). “Report on Gareloi (United States),” in *Weekly Volcanic Activity Report, 28 July-3 August 2021*. Editor S. K. Sennert (Washington, DC: Smithsonian Institution and US Geological Survey). doi=GVP.WVAR20210728-311070.
- GVP (2021c). “Report on Pavlof (United States),” in *Weekly Volcanic Activity Report, 18 August-24 August 2021*. Editor S. K. Sennert (Washington, DC: Smithsonian Institution and US Geological Survey). doi=GVP.WVAR20210818-312030.
- GVP (2021d). “Report on Semisopochnoi (United States),” in *Bulletin of the Global Volcanism Network*. Editors J. B. Krippner and E. Venzke (Washington, DC: Smithsonian Institution), 46, 6. doi:10.5479/si.GVP.BGVN202106-311060
- GVP (2019). “Report on Great Sitkin (United States),” in *Bulletin of the Global Volcanism Network*. Editor E. Venzke (Smithsonian Institution), 44, 7. doi:10.5479/si.GVP.BGVN201907-311120
- Henley, R. W., and Fischer, T. P. (2021). Sulfur Sequestration and Redox Equilibria in Volcanic Gases. *J. Volcanology Geothermal Res.* 414, 107181. doi:10.1016/j.jvolgeores.2021.107181
- Hilton, D. R., Fischer, T. P., and Marty, B. (2002). “9. Noble Gases and Volatile Recycling at Subduction Zones,” in *MSA Special Volume: Noble Gases in Geochemistry and Cosmochemistry*. Editors D. Porcelli, C. Ballentine, and R. Wieler, 47, 319–370. doi:10.1515/9781501509056-011
- Hilton, D. R., Fischer, T. P., McGonigle, A. J. S., and de Moor, J. M. (2007). Variable SO<sub>2</sub> Emission Rates for Anatahan Volcano, the Commonwealth of the Northern Mariana Islands: Implications for Deriving Arc-wide Volatile Fluxes from Erupting Volcanoes. *Geophys. Res. Lett.* 34. doi:10.1029/2007GL030405
- Ilanco, T., Fischer, T. P., Kyle, P., Curtis, A., Lee, H., and Sano, Y. (2019). Modification of Fumarolic Gases by the Ice-Covered Edifice of Erebus Volcano, Antarctica. *J. Volcanol. Geotherm. Res.* 381, 119–139. doi:10.1016/j.jvolgeores.2019.05.017
- Kelemen, P. B., Yogodzinski, G. M., and Scholl, D. W. (2003). Along-strike Variation in the Aleutian Island Arc: Genesis of High Mg# Andesite and Implications for continental Crust. *Geophys. Monogr.* 138, 223–276. doi:10.1029/138gm11
- Kraus, S. (2006). DOASIS a Framework Design for DOAS. Ph.D. Thesis Thesis (Mannheim: Universitaet Mannheim).
- Larsen, J. F., Neal, C. A., and Cameron, C. E. (2020). Major-oxide and Trace-Element Geochemical Data from Rocks Collected on Little Sitkin Island, from Little Sitkin Volcano, Alaska. *Alsk. Division Geol. Geophys. Surv. Raw Data File 2020-4*, 4. doi:10.14509/30440
- Lee, H., Fischer, T. P., Muirhead, J. D., Ebinger, C. J., Kattenhorn, S. A., Sharp, Z. D., et al. (2017). Incipient Rifting Accompanied by the Release of Subcontinental Lithospheric Mantle Volatiles in the Magadi and Natron basin, East Africa. *J. Volcanology Geothermal Res.* 346, 118–133. doi:10.1016/j.jvolgeores.2017.03.017
- Li, L., Bebout, G. E., and Idleman, B. D. (2007). Nitrogen Concentration and δ<sup>15</sup>N of Altered Oceanic Crust Obtained on ODP Legs 129 and 185: Insights into Alteration-Related Nitrogen Enrichment and the Nitrogen Subduction Budget. *Geochimica et Cosmochimica Acta* 71, 2344–2360. doi:10.1016/j.gca.2007.02.001
- Lopez, T., Tassi, F., Aiuppa, A., Galle, B., Rizzo, A. L., Fiebig, J., et al. (2017). Geochemical Constraints on Volatile Sources and Subsurface Conditions at Mount Martin, Mount Mageik, and Trident Volcanoes, Katmai Volcanic Cluster, Alaska. *J. Volcanology Geothermal Res.* 347, 64–81. doi:10.1016/j.jvolgeores.2017.09.001
- Martin, R. S., Mather, T. A., and Pyle, D. M. (2006). High-temperature Mixtures of Magmatic and Atmospheric Gases. *Geochem. Geophys. Geosyst.* 7, Q04006. doi:10.1029/2005gc001186
- Marty, B., and Jambon, A. (1987). C<sub>3</sub>H<sub>6</sub> in Volatile Fluxes from the Solid Earth: Implications for Carbon Geodynamics. *Earth Planet. Sci. Lett.* 83, 16–26. doi:10.1016/0012-821x(87)90047-1
- McGee, K. A., Doukas, M. P., McGimsey, R. G., Neal, C. A., and Wessels, R. L. (2010). “Emission of SO<sub>2</sub>, CO<sub>2</sub>, and H<sub>2</sub>S from Augustine Volcano, 2002–2008: Chapter 26 in the 2006 Eruption of Augustine Volcano, Alaska,” in *The 2006 Eruption of Augustine Volcano, Alaska*. Editors J. Power, M. Coombs, and J. Freymueller (Reston, Virginia: U.S. Geological Survey Professional Paper 1769), 609–627. doi:10.3133/pp176926



- Miller, T. P., McGimsey, R. G., Richter, D. H., Riehle, J. R., Nye, C. J., Yount, M. E., et al. (1998). Catalog of the Historically Active Volcanoes of Alaska. U.S. Geological Survey Open-File Report 98-0582. Reston, Virginia: U.S. Geological Survey, 104.
- Mitchell, E. C., Fischer, T. P., Hilton, D. R., Hauri, E. H., Shaw, A. M., de Moor, J. M., et al. (2010). Nitrogen Sources and Recycling at Subduction Zones: Insights from the Izu-Bonin-Mariana Arc. *Geochem. Geophys. Geosyst.* 11, a–n. doi:10.1029/2009GC002783
- Motyka, R. J., Liss, S. A., Nye, C. J., and Moorman, M. A. (1993). *Geothermal Resources of the Aleutian Arc*. Reston, Virginia: USGS Professional Report, 114.
- Oppenheimer, C., Fischer, T. P., and Scaillet, B. (2014). Volcanic Degassing: Processes and Impact. *Treatise Geochem.* 4, 111–179. doi:10.1016/B1978-1010-1008-095975-095977.000304-095971
- Plank, T., and Langmuir, C. H. (1998). The Chemical Composition of Subducting Sediment and its Consequences for the Crust and Mantle. *Chem. Geology*. second edition 145, 325–394. doi:10.1016/s0009-2541(97)00150-2
- Rizzo, A. L., Caracausi, A., Chavagnac, V., Nomikou, P., Polymenakou, P. N., Mandalakis, M., et al. (2016). Kolumbo Submarine Volcano (Greece): An Active Window into the Aegean Subduction System. *Sci. Rep.* 6, 28013. doi:10.1038/srep28013
- Rizzo, A. L., Jost, H. J., Caracausi, A., Paonita, A., Liotta, M., and Martelli, M. (2014). Real-time Measurements of the Concentration and Isotope Composition of Atmospheric and Volcanic CO<sub>2</sub> at Mount Etna (Italy). *Geophys. Res. Lett.* 41, 2382–2389. doi:10.1002/2014gl059722
- Sano, Y., and Fischer, T. P. (2013). “The Analysis and Interpretation of noble Gases in Modern Hydrothermal Systems,” in *Noble Gases as Geochemical Tracers (Peter Burnard, Editor)*. Series: *Advances in Isotope Geochemistry*. Editors J. Hoefs (Heidelberg: Springer-Verlag). ISBN 978-3-642-28835-7. doi:10.1007/978-3-642-28836-4\_10
- Sano, Y., Gamoto, T., and Williams, S. N. (1997). Secular Variations of Helium and Carbon Isotopes at Galeras Volcano, Colombia. *J. Volcanology Geothermal Res.* 77, 255–265. doi:10.1016/s0377-0273(96)00098-4
- Sano, Y., and Marty, B. (1995). Origin of Carbon in Fumarolic Gas from Island Arcs. *Chem. Geology*. 119, 265–274. doi:10.1016/0009-2541(94)00097-r
- Sano, Y., Takahata, N., Nishio, Y., Fischer, T. P., and Williams, S. N. (2001). Volcanic Flux of Nitrogen from the Earth. *Chem. Geology*. 171, 263–271. doi:10.1016/s0009-2541(00)00252-7
- Shinohara, H. (2013). Volatile Flux from Subduction Zone Volcanoes: Insights from a Detailed Evaluation of the Fluxes from Volcanoes in Japan. *J. Volcanology Geothermal Res.* 268, 46–63. doi:10.1016/j.jvolgeores.2013.10.007
- Snyder, G. L. (1959). Geology of Little Sitkin Island, Alaska. In *Investigations of Alaskan Volcanoes*. U.S. Geological Survey Bulletin 1028-H. Reston, Virginia: U.S. Geological Survey, 169–210.
- Stoiber, R. E., Malinconico, L. L. J., and Williams, S. N. (1983). “Use of the Correlation Spectrometer at Volcanoes,” in *Forecasting Volcanic Events*. Editors H. Tazieff and J. Sabroux (New York: Elsevier), 425–444.
- Symonds, R. B., Janik, C. J., Evans, W. C., Ritchie, B. E., Counce, D., Poreda, R., et al. (2003a). Scrubbing Masks Magmatic Degassing During Repose at Cascade-Range and Aleutian-Arc Volcanoes. USGS Open File report, 03-435. Reston, Virginia: U.S. Geological Survey.
- Symonds, R. B., Poreda, R. J., Evans, W. C., and Janik, C. J. (2003b). Mantle and Crustal Sources of Carbon, Nitrogen, and noble Gases in Cascade-Range and Aleutian-Arc Volcanic Gases. U.S. Geological Survey Open-File Report 03-436. Reston, Virginia: U.S. Geological Survey.
- Taran, Y. A. (2009). Geochemistry of Volcanic and Hydrothermal Fluids and Volatile Budget of the Kamchatka-Kuril Subduction Zone. *Geochimica et Cosmochimica Acta* 73 (4), 1067–1094. doi:10.1016/j.gca.2008.11.020
- Taran, Y., Zelenski, M., Chaplygin, I., Malik, N., Campion, R., Inguaggiato, S., et al. (2018). Gas Emissions from Volcanoes of the Kuril Island Arc (NW Pacific): Geochemistry and Fluxes. *Geochem. Geophys. Geosyst.* 19, 1859–1880. doi:10.1029/2018gc007477
- Taran, Y., and Zelenski, M. (2015). Systematics of Water Isotopic Composition and Chlorine Content in Arc-Volcanic Gases. *Geol. Soc. Lond. Spec. Publications* 410 (1), 237–262. doi:10.1144/sp410.5
- Tolstikhin, I. N. (1986). *Isotope Geochemistry of Helium Argon and Rare Gases*. Leningrad: Nauka, 200. in Russian.
- Werner, C. A., Doukas, M. P., and Kelly, P. J. (2011). Gas Emissions from Failed and Actual Eruptions from Cook Inlet Volcanoes, Alaska, 1989–2006. *Bull. Volcanol* 73, 155–173. doi:10.1007/s00445-011-0453-4
- Werner, C., Evans, W. C., Poland, M., Tucker, D. S., and Doukas, M. P. (2009). Long-term Changes in Quiescent Degassing at Mount Baker Volcano, Washington, USA; Evidence for a Stalled Intrusion in 1975 and Connection to a Deep Magma Source. *J. Volcanology Geothermal Res.* 186 (3-4), 379–386. doi:10.1016/j.jvolgeores.2009.07.006
- Werner, C., Fischer, T. P., Aiuppa, A., Edmonds, M., Cardellini, C., Carn, S., et al. (2019). “Carbon Dioxide Emissions from Subaerial Volcanic Regions,” in *Deep Carbon: Past to Present*. Editors B. N. Orcutt, I. Daniel, and R. Dasgupta (Cambridge, United Kingdom: Cambridge University Press). doi:10.1017/9781108677950.008
- Werner, C., Kelly, P. J., Doukas, M., Lopez, T., Pfeffer, M., McGimsey, R., et al. (2013). Degassing of CO<sub>2</sub>, SO<sub>2</sub>, and H<sub>2</sub>S Associated with the 2009 Eruption of Redoubt Volcano, Alaska. *J. Volcanology Geothermal Res.* 259, 270–284. doi:10.1016/j.jvolgeores.2012.04.012

**Conflict of Interest:** The authors declare that the research was conducted in the absence of any commercial or financial relationships that could be construed as a potential conflict of interest.

**Publisher’s Note:** All claims expressed in this article are solely those of the authors and do not necessarily represent those of their affiliated organizations, or those of the publisher, the editors and the reviewers. Any product that may be evaluated in this article, or claim that may be made by its manufacturer, is not guaranteed or endorsed by the publisher.

Copyright © 2021 Fischer, Lopez, Aiuppa, Rizzo, Ilanko, Kelley and Cottrell. This is an open-access article distributed under the terms of the Creative Commons Attribution License (CC BY). The use, distribution or reproduction in other forums is permitted, provided the original author(s) and the copyright owner(s) are credited and that the original publication in this journal is cited, in accordance with accepted academic practice. No use, distribution or reproduction is permitted which does not comply with these terms.